Rebuttal for tc-2019-285

Takehiko Nose on behalf of all authors

Overview of major changes

We begin with an overview of major changes in the revised manuscript to address both reviewers' comment regarding readability of the paper. The change of section titles is shown in bold text (if changed).

Abstract The abstract has been rewritten to more clearly emphasise the focus of the study and its findings.

Section 2.3 The description of WAVEWATCH III ® (WW3) has been modified in a way that it is focused on the core idea of the paper: wave-ice interactions. The readability is improved by using equations and compact notations, thereby demonstrating clearly the link between sea ice concentration (SIC) and wave-ice models. Please see the modified Section 2.3 starting at P5L142 (i.e., page 5 line 142) of the revised manuscript.

Section 3 Sea ice concentration: definition, characteristics, and the use in wave-ice models

The presentation of this section is one of the major changes in the revised version. We have rewritten this section to discuss the concept of SIC from a wave-ice modelling perspective. Despite different scales and objectives, the SIC is being used to moderate the attenuation rate of waves in the MIZ without the model having any consideration to the sea ice field heterogeneity, i.e., subgrid scale physics. We discuss the implication of the length scale of satellite retrieved SIC to the SIC and wave-ice model formulation. Please see the modified Section 3 starting at P7L205 of the revised manuscript.

Section 3.2 is shortened and moved to the beginning of Section 5 (P10L284 of the revised manuscript) to give an overview of how satellite retrieved SIC varies on a regional scale so that the transition to the wave hindcast analysis of the region is more fluent.

Original Figures 3 and 4 are removed as they were deemed unnecessary.

Section 4 Δc_i effects on wave modelling at the observation sites

Note Δc_i is denoted as the SIC uncertainty in the text.

Section 5 Δc_i and wave modelling in the refreezing Chukchi Sea

Section 5.1 On- and off-ice wave evolution in the refreezing Chukchi Sea MIZs

Section 5.2 Relative significance of Δc_i compared with wave-ice interaction parameterisation uncertainty

We tested the robustness of the results based on sensitivity analyses that tested sea ice thickness (SIT) and the inclusion of scattering. The study findings remain unchanged. Please see the revised manuscript P12L383–P13L398.

Section 6 Conclusions and discussions

This section is shortened considerably and includes discussions on the study outcome. Please see the revised manuscript P13L403–P14L420.

Reviewer #1 General comments

Reviewer comment R#1-1 This paper presents interesting results, confirming some statements about the sensitivity of wave-inice modelling to sea ice concentration made in previous studies. The fact that the uncertainty in the estimated sea ice concentration has a larger effect on the uncertainty of the wave height estimated in-ice than the change in the wave-in-ice attenuation parameterization is a nice finding that illustrates very well the difficulties faced by wave-in-ice modellers. However, the paper suffers from a writing style that is confusing in a number of places. This is particularly the case for sections 3, 4 and 5. It is a bit paradoxal, as sometimes the important information is hidden in a succession of very wordy sentences, making it hard for the reader to get the message, and sometimes it seems that the authors wanted to avoid repeating themselves whereas the reader would happily appreciate some help.

Author response We are pleased the essence of this manuscript was conveyed to the reviewer. To enhance the clarity of our message, efforts were made to improve the readability of the paper by following reviewer's suggestions. Please see the overview of major changes.

Reviewer comment R#1-2 I am also not convinced by the usefulness and the novelty of section 3, at least in its current form. To me, the most interesting part of the study lies in section 5, but it is overshadowed by the lack of clarity of the previous sections. It would be worth shifting the emphasis of the paper to this section more quickly.

Author response We appreciate the critical comment regarding the Section 3 content. Please see the overview of major changes and the modified Section 3 starting at P7L205 of the revised manuscript.

Reviewer #1 Specific comments

Reviewer comment R#1-3 : P1L22. "model uncertainties...", which models are the authors talking about here?

Author response We made a change to this passage. Please see the revised manuscript P1L22–P2L27.

Reviewer comment R#1-4 : P2L25. The authors should consider giving a definition of the MIZ.

Author response The MIZ definition is added. Please see the revised manuscript P2L29–31.

Reviewer comment R#1-5 : P2L36. "wave-ice interaction source term": the authors haven't introduced the principle of spectral wave models yet, so it is not clear for everyone what the wave-ice interaction source term is.

Author response Changed the object from "the wave-ice interaction source term" to "the wave-ice interaction parameterisation". Please see the revised manuscript P2L37.

Reviewer comment R#1-6 : P3L64. Here the authors introduce the methods used for the measurements on board on the R/V Mirai. But the way the so called "sea truth" images were taken is only described in section 3.1 (P7L212), lost in comments on the results. Similarly, before the end of section 3.1, a definition of how the uncertainty of a given quantity is computed is suddenly introduced, without even a proper transition (P8L225). This mix between comments on the results and details of the methods makes section 3.1 very confusing and much longer than it should be.

Author response Please see author's response to R#1-2. Regarding the uncertainty definition, it is moved to Section 2.2 and introduced where the eight SIC products are described. Please see the revised manuscript P4L113.

Reviewer comment R#1-7 : P4L88. I think the word "translated" is not appropriate here (and in some other places). The authors could consider using "interpreted", "inferred".

Author response SIC is a variable that is calculated from brightness temperatures, so we would prefer to have a quantitative phrase rather than being qualitative. In that sense, "calculate" is more appropriate here. Please see the revised manuscript P4L101. Regarding the use of "translate" in other places, we have replaced them with more straightforward expressions.

Reviewer comment R#1-8 : P4L118. The sentences about the different grids the authors could have used and the one they are actually using are really confusing. Maybe they should try to cut them into more but shorter sentences, each dealing with one region and one resolution.

Author response Changed to a shorter sentence as suggested. Please see the revised manuscript P5L130–133.

Reviewer comment R#1-9 : P5L143. "A curvilinear grid [...] sea point cells." I found this whole paragraph very confusing. As a reader I found very difficult to understand the links between each sentence, and the expression "The grid" seems to be applied to different things. As an example, they first refer to the model "geographical" grid, then to the spectral grid, then they use again the expression "the grid" to give details about the bathymetry. A quick reminder of the region they are focusing on would also be welcome, especially as they refer to the "other seas" at the border of "the domain".

Author response Adding appropriate modifiers to "grid" was necessary, and the spectral grid description was mixed up in the regional grid description, which was confusing. The paragraph is clarified and shortened. Please see the revised manuscript P7L185–189.

Reviewer comment R#1-10 : P6L152. "During the version upgrade of TodaiWW3-ArCS...": which version upgrade are the authors referring to? Are they sure it is relevant for the paper? I think the authors could just state that they are using the ST6 parameterization for the non-ice source terms as it was previously shown to give the best results for the case discussed in Nose et al. (2018) with the model being forced by ERA5 winds.

Author response Corrected as suggested. Please see the revised manuscript P6L179–184.

Reviewer comment R#1-11 : P6L157. "The s_ice term is composed": I think the use of composed is misleading here. The attenuation terms the authors mention are included in different parameterizations (ISX, ICX), and they are not all compatible with each other. I would suggest an expression like "The s_ice term represents wave-in-ice attenuation processes such as..." for instance.

Author response The passage relating to the WW3 wave-ice interaction term is one of the major changes. Please see the revised manuscript P6L154–171.

Reviewer comment R#1-12: P6L160. "The dominant floe size [...] IS0 switch.": Here I have the feeling that the authors want to justify why they did not include scattering terms in their wave-in-ice source terms. I think this justification is very long and with unnecessary information (the way scattering terms work in WW3 for instance). I think it would be much clearer simply stating that during the cruise, sea ice in the MIZ was mainly made of grease, nilas and pancake ice, for which scattering is not expected to be the dominant process (Montiel et al., 2018), and therefore scattering was not considered here. Specifying the WW3 switch IS0 is also unnecessary.

Author response Thank you for this suggestion. The suggested text is succinct and used in the manuscript. Please see the revised manuscript P6L174.

Reviewer comment R#1-13: P6L170. "The underlying principle of sea ice models is that sea ice is treated a continuum." Firstly, there is a small typo, it should be "treated as...". Secondly, this statement might be true for the sea ice models used in climate models, but it ignores discrete elements

sea ice models, often used for sea ice-structure interactions. They can also be used to study wave-ice interactions (Herman et al., 2015). Actually I think the sentences between P6L170 and P6L173 could be shortened. The reason the authors choose this parameterization is because it has been developed to represent similar ice conditions to the ones encountered by the R/V Mirai, which is not the case for the other parameterizations.

Author response We have incorporated the reviewer's comment. Please see the revised manuscript P6L172.

Reviewer comment R#1-14: P6L175. "... the treatment of independent SIC and sea ice thickness data sets is not a trivial matter." I am not sure I understand this statement. Would it be possible to develop this idea a bit more?

Author response It is much clearer just to say the constant thickness was applied, so we can evaluate solely the SIC uncertainty on wave modelling. The text is modified. Please see the revised manuscript P6L175–178.

Reviewer comment R#1-15: P6L179. "the former [...] experiment." The first part of the sentence is unnecessary in my opinion. I would also recommend avoiding using the word "domain" for the the SIC product, as it usually refers to the study region.

Author response Corrected as suggested. Please see the revised manuscript P7L190–192.

Reviewer comment R#1-16: P6L184 . "By doing so [...] in atmospheric models." This passage is very confusing, I do not understand the point the authors are trying to make. They should either rewrite it, if they think it is important, or remove it.

Author response The passage is rewritten. Please see the revised manuscript P7L198–203.

Reviewer comment R#1-17: P7L189. "WW3 is a standalone wave model...": In this case, it is indeed used in standalone mode, but WW3 can be coupled.

Author response This is true the modifier "standalone" was unnecessary. Further, the entire sentence turned out to be superfluous when we addressed R#1-16, and as such, the sentence is removed.

Reviewer comment R#1-18: P7L190. "numerical stability is unaffected": By what?

Author response This sentence is removed. Please see author's responses to R#-16 and R#-17.

Reviewer comment R#1-19: P7L195, Section 3. I am not particularly convinced by the major interest of this section, and particularly by the interest of comparing pictures taken from the boat to the sea ice concentration products in section 3.1. Which angle does the pictures cover? Which surface area are they representative of? As the authors say, sea ice tends to cluster in the MIZ, and the fact that the sea ice concentration is not uniformly distributed spatially is well known by anyone who has had the opportunity to go in sea ice covered places. As I understand it, these observations motivated the study, but to me the interest of this paper does not lie here, and I actually think the removal of section 3.1 could potentially improve the clarity of the paper. If the authors want to keep it, they must make clearer the novelty of these observations and their interest. Moreover, I find the writing style very confusing in section 3.1. Section 3.2 is more convincing and clearer, but it is hard to see any novelty in it. It could maybe bring more to the study by linking it more closely to the results of section 4 and 5.

Author response Please see the overview of major changes and author's response to R#1-2.

Reviewer comment R#1-20: P7L197. I don't understand the use of "respectively" here.

Author response This passage is moved to an appendix, and the "respectively" is removed there. Please see the revised manuscript P16L482.

Reviewer comment R#1-21: P9L270. "... the sea ice cut-off criterion is not clear in the documentation." This is not a very satisfying statement. Have the authors considered contacting the people in charge of ArcMFC to get more information about this criterion?

Author response Thank you for this comment: the statement was unsatisfactory. We found out that the wave-ice interaction of Sutherland et al. [2019] was implemented in December, 2019: the month after our Arctic Ocean observation. We still find value in reporting the ARCMFC model data in our results, but we have amended the ARCMFC model description. Please see the revised manuscript P8L233.

Reviewer comment R#1-22: P9L275. "... but the Piper [...] did not reflect the sea state.": It is quite confusing, please rephrase.

Author response Waves in the Chukchi Sea during the study period was dominated by wind seas, which have shorter wavelength relative to the ship dimensions. These short waves are impeded by R/V Mirai's hull, so the shipboard Piper#15 has limitations on measuring wind seas. As such, most of the Piper#15 data did not reflect the true wave field. We have rephrased the paragraph, and the explanation of this point is moved to an appendix. So it is removed from the main text. Please refer to author's response to R#1-34 for how we addressed this comment.

Reviewer comment R#1-23: P9L283. "Furthermore [...] an important role." This is very noticeable indeed. It would be very interesting to give an estimate of the spatial attenuation coefficient at the ice edge assuming an exponential wave attenuation, in order to show how it compares with the models and other reported observations (for instance Kohout et al., 2015).

Author response Thank you for the comment. We realised we used incorrect expressions to describe the wave height uncertainty earlier in this paragraph, which likely led the reviewer to inquire about the attenuation rates. In P9L278 of the original manuscript, we stated "waves decay with varying attenuation rates"; however, this is changed to "waves decay at different timing depending on the sea ice edge location of the respective SIC forcing used" (P8L244 in the revised manuscript). The whole point of the experiment is testing different SIC forcing using the consistent wave-ice interaction source term setting, i.e., the same attenuation coefficient. We apologise for the misleading sentence.

We are also mindful that a successful study of wave attenuation rates depends strictly on the knowledge of the ice edge or availability of two and more buoys along the fetch. As such, we are unable to repeat the novel analysis of Kohout et al. [2016] because we did not have enough measurements along the fetch.

Reviewer comment R#1-24: P11L343. I don't think that one can write that the MIZ is aligned with the wind. The MIZ is an area. Maybe the authors could substitute MIZ by "the ice edge".

Author response The sentence is corrected by replacing "MIZs" with "ice edges" (P11L320 in the revised manuscript).

Reviewer comment R#1-25: P12L352. "The figure only comprising...": I don't understand this sentence. What does "highly forced waves" mean?

Author response Highly forced waves imply a wave field, specifically wind seas, that is rapidly growing under the wind forcing. The sentence is rewritten to clarify the point. Please see the revised manuscript P11L329.

Reviewer comment R#1-26: P12L362. "this can occur": What is "this"?

Author response "this" is specified as "high ΔH_{m0}". Please see the revised manuscript P11L338.

Reviewer comment R#1-27: P12L365. "Here, ..." I don't understand this sentence either, please consider rephrasing it.

Author response In this sentence, "highly forced" was unnecessary and is removed. The subject of the sentence is also clarified instead of using "Here". Please see the revised manuscript P11L341-343.

Reviewer comment R#1-28: P12L371. "The off-ice [...] of Appendix D." These two paragraphs are very confusing in my opinion, mostly because they are not well structured. It makes it very hard for the reader to understand the problem the authors are trying to address. They should be entirely rewritten.

Author response The repeat introduction of the equation in both paragraphs made them seem unstructured. We also made the second paragraph more succinct. The two paragraphs are modified. Please see the revised manuscript P11L346–P12L360.

Reviewer comment R#1-29: P13L405. "Three principal parameters that form the sea ice forcing are": This formulation is misleading. I would instead say: "The three main parameters used to tune the wave-in-ice attenuation in the IC2,IC3 and IC5 parameterizations are"

Author response The sentence is changed as suggested. Please see the revised manuscript P12L370.

Reviewer comment R#1-30: P14L421. "The values here [...] the adopted default source term parameters." I am not sure I understand this sentence, it should be rewritten.

Author response This sentence was unnecessary and is removed.

Reviewer comment R#1-31: P14L422 . "Our analysis demonstrates..." This statement should be at least discussed a bit more. For instance, the authors have used a limited number of wave-in-ice attenuation parameterizations, and none of them represent the wave scattering. Also, could these results change in a MIZ made of large floes and thicker ice for example? In addition, the authors have assumed a constant sea ice thickness of 10cm, and it is known that the behaviour of attenuation processes can change significantly depending on the sea ice thickness (see for instance Boutin et al., 2018). The sensitivity of these results to the sea ice thickness should be explored and discussed, for example by setting it to 20/30cm instead of 10cm.

Author response Agreed that further discussion is warranted. We tested robustness of the study finding by checking sensitivity to SIT and scattering. Please see the revised manuscript P12L383–P13L398.

Reviewer comment R#1-32: P14L422 . The conclusion is, in my opinion, much longer than it should be. I think it would have more impact if the results were synthesized in a few sentences only, and if it was ending with a discussion on the perspestives and the consequences of the findings presented here.

Author response The conclusion section has been made more succinct. Please see the revised manuscript P13L403–P14L420.

Reviewer comment R#1-33: P14L443. "Reliable modelling [...] melt the Arctic Ocean sea ice." I don't really see the cause/consequence link in this sentence.

Author response The sentence is removed as it was unnecessary. See author's changes in manuscript to R#1-32.

Reviewer comment R#1-34: P16L490. "Reliable shipboard [...] was slow." I find the formulations used in these sentences a bit ambiguous. For instance, what do the authors mean by "seemingly sensible"? I think I get the idea, but it is not very clearly expressed. It is also not clear to me what is validated in the first sentence.

Author response How these data were used in the study is described with more clarity. We have rewritten this passage in Appendix A explaining how the shipboard data were used. Please see the

revised manuscript P14L426–442.

Reviewer comment R#1-35: P25 Figure 4. "showing considerable uncertainty": This comment should be in the main text, not in the caption. The font size of the legend is also too small.

Author response The figure is removed as described in the overview of major changes.

Reviewer #1 Technical corrections

Reviewer comment R#1-36: General. I would recommend using a roman text font for the subscripts that are made of more than one character in the equations (low in f_low) for instance (If you are using latex, it means that you should add "\rm" or "\mathrmmy_subscript" in your equations). It would improve the readability of the paper.

Author response Subscripts are changed to roman text as recommended.

Reviewer comment R#1-37: P1L21. "encountering high winds...": encounters is already the verb of the sentence, so no need to repeat.

Author response Removed the verb phrase. Please see author's changes to manuscript in R#1-3.

Reviewer comment R#1-38: P6L174. "Sea thickness"→"Sea ice thickness"

Author response Corrected.

Reviewer comment R#1-39: P14L440. "have"→"has".

Author response Corrected.

Reviewer comment R#1-40: P15L478. ":microwave..."→":a microwave...".

Author response Corrected.

Reviewer comment R#1-41: P15L480. "a variant but similar device of Kohout et al..."→"a device similar to the one used by Kohout et al. (2015)".

Author response Changed as suggested.

Reviewer #2 General comments

Reviewer comment R#2-1 The manuscript examines the impact of observational uncertainty in sea ice concentration on numerical modelling of ocean surface waves in sea ice, using Wavewatch III. The most interesting finding, in my opinion, is that the effect of this uncertainty on wave modelling is large, and larger than the differences between various wave-ice interaction source terms currently included in WW3.

In general, I find the results to be well supported by thorough analysis. The manuscript is a little hard to follow in places (some instances of this noted below in 'presentational comments'). As currently presented, my sense is that this work is of interest to a narrow section of the community (i.e. those working on spectral models of wave-ice interactions) and may be better suited to a more targeted journal. However, this could be addressed by revising the text to stress the aspects that could be interesting to a more general audience e.g. the differences between SIC products and their accuracy near the ice edge; that the sea ice coverage may be more important in determining ocean surface waves in ice than a detailed understanding of wave-ice interaction physics; the level to which waves in the open ocean are influenced by sea ice.

Author response We are pleased the significance of the SIC uncertainty on wave-ice models has been conveyed to the reviewer. Regarding the suggested approach to broaden the audience (*"e.g. the differences between SIC products and their accuracy near the ice edge; that the sea ice coverage may be more important in determining ocean surface waves in ice than a detailed understanding of wave-ice interaction physics; the level to which waves in the open ocean are influenced by sea ice"*), our analysis aims to convey that wave-ice model tuning may not be as effective at this time when the knowledge of the true SIC field is too uncertain; however, our work was not intended to suggest that SIC forcing accuracy takes precedence over the detailed understanding of wave-ice interaction physics. Our view is that advancing the knowledge of wave-ice interactions and its implementation in WW3 (or other wave model platforms) constitute the foundation to improving the predictability of ocean waves in ice-covered waters.

The research of ocean waves are becoming an important polar region research topic; waves feedback to the dynamics of atmosphere, ocean, and sea ice, and as such, we believe the manuscript contents are of interest to a general audience of The Cryosphere (TC). The recent acceptance of a coupled ice-ocean-wave model paper [Boutin et al., 2019] in TC reflects the increasing interest of the audience to the topic of ocean waves. We also cited the coupled wave-ice model references in the text to address R#2-10, which should help attract a wider audience.

Reviewer #2 Major comments

Reviewer#2 comment R#2-2 'Analysis of significant wave height uncertainty distributions for SIC forcing and wave-ice interaction source terms reveals that they are both sizeable; however, the study concludes the more dominant uncertainty source of modelling wave-ice interactions is the accuracy of satellite retrieved SIC estimates that are used as model forcing.' The authors need to clarify that uncertainty in wave-ice interaction terms is an estimate based only on the various wave-ice interaction terms included in WW3, which as the authors note later in the manuscript are based on a limited number of field observations. It does not sample all possible wave-ice interaction terms, nor does it sample different parameter values.

Author response Abstract has been rewritten as mentioned in the overview of major changes. Please see the revised manuscript P1L1–14.

Reviewer comment R#2-3 It is well-known that SIC satellite observations underestimate concentrations for low thicknesses, less than 35 cm (Ivanova et al. 2015). This should be stated in the Introduction. I think the newer result here is how varied the satellite products are for these low thicknesses. This should be made clearer in the text.

Author response The long-known deficiency of satellite derived SIC accuracy in thin ice was in-

deed missing. We have incorporated the comment in Section 1 Introduction. Please see the revised manuscript P2L56.

Reviewer comment R#2-4 Sec 2.3 This section needs more explanation to make it suitable for a more general audience - i.e. those not familiar with WW3 wave-ice interaction terms. What is the IS0 switch?

Author response We have modified Section 2.3 to be more readable to a broader audience. Please see the overview of major changes and the modified Section 2.3 starting at P5L142 of the revised manuscript.

Reviewer comment R#2-5 What is the estimated of spatial domain of the sea-truth concentration observations? Are these comparable to the resolution of the satellite products?

Author response Here, we infer the comment pertains to Section 3.1. This section has been rewritten to address Reviewer#1's comments (refer to R#1-1, R#1-2, and R#1-19). Please see the modified Section 3 starting at P7L205 of the revised manuscript.

Reviewer comment R#2-6 Sec 3.2 - why are only three products considered here? Conclusions on which products perform best (or worst) for this region would be useful and of broader interest to the cryospheric community.

Author response The three products were selected to convey the magnitude of uncertainty. Since the uncertainty was defined as $\Delta c_i = max(c_i) - min(c_i)$, three products are sufficient to convey this point. Showing all eight products clutters the figure and potentially distract readers from the main point. Note that this sub-section is moved to Section 5 (P10L284 of the revised manuscript).

In addition, the revised manuscript is presented such that the focus is apparent, which is the wave-ice models and SIC forcing and not about the SIC data. We anticipate this will be apparent when the revised manuscript is read. Nevertheless, regarding ranking the product performance, we agree such a conclusion would be a significant contribution. We have attempted to rank the SIC products, but the result is inconclusive primarily due to the number of days comprehensive mosaic can be produced and inconsistent variability of SIC estimates. We expect such an analysis warrants a separate dedicated study to produce noteworthy outcomes, especially considering the previous intercomparison studies, such as Ivanova et al. [2015] and Comiso et al. [2017], concluded there is no one product that is superior. They state that the choice of SIC products are largely dictated by the SIC data application, and we concur with this statement based on our field observation and analysis conducted.

Reviewer #2 Minor comments

Reviewer comment R#2-7 : L22. 'which are greater in the Arctic regions.' As compared to what?

Author response We made a change to this passage. Please see the revised manuscript P1L22–P2L27.

Reviewer comment R#2-8 : L23. 'sustainable developments of the Arctic Ocean' - this statement sounds strange.

Author response Please see author response to R#2-7.

Reviewer comment R#2-9 : L28. 'dispersion relation'→'the dispersion relation'.

Author response Corrected.

Reviewer comment R#2-10: L32. Other recent work on wave-ice interactions could be cited here: Zhang et al. 2019 (https://doi.org/10.1016/j.ocemod.2019.101532), Roach et al. 2019

(https://doi.org/10.1029/2019MS001836).

Author response This passage pertains specifically to the standalone WW3 wave-ice interaction source term developments, so the suggested references are unrelated. We added new sentences to address this comment at the end of the paragraph. This way, we can relate the study to a broader audience, which also helps to address R#2-1. Please see the revised manuscript P2L42–L45.

Reviewer comment R#2-11 : L37. 'Besides the model interior' What does this mean?

Author response We are referring to the inner part of numerical models. We added "wave-ice interaction parameterisations" as an example. Please see the revised manuscript P2L46.

Reviewer comment R#2-12: L37. 'like SIC'→'in products such as SIC'?

Author response Changed as suggested.

Reviewer comment R#2-13: L69. 'generally'→'generally between'.

Author response Corrected.

Reviewer comment R#2-14: L70. 'Albeit the MIZ coverage..' - this sentence is unclear.

Author response We have attempted to make it clearer. Please see the revised manuscript P3L84–86.

Reviewer comment R#2-15: L82. 'mostly same'→'mostly the same'.

Author response Corrected.

Reviewer comment R#2-16 : L96. remove 'exhaustive' (this is an opinion).

Author response "exhaustive" changed to "large".

Reviewer comment R#2-17 : L102. 'most frequent'→'most frequently'.

Author response Changed as suggested.

Reviewer comment R#2-18 : L102. 'leading algorithms' leading in what? Perhaps you mean the most commonly used?.

Author response We realised the phrase is unnecessary, so it is removed.

Reviewer comment R#2-19 : L152. 'sanity checked' inappropriate language for a publication.

Author response Changed to "tested". Please see the revised manuscript P6L179.

Reviewer comment R#2-20 : L153. 'leading packages' again, leading in what way? Most commonly used? Most skill?.

Author response Changed to "commonly used".

Reviewer comment R#2-21 : L211. change to 'SSTs exceeded 0oC'.

Author response Corrected. Please see the revised manuscript P16L495.

R#2-22 : L211. At what depth were the shipboard SSTs measured? Are they affected by the ship itself?.

Author response The technical details of the instruments were given in Appendix A, which was introduced in L76 of the original version: "−1 m below the sea surface with further 5 m inlet to the gauge" (L458). We are not aware of any ship effects on the SST measurement. During the cruise,

we note that sea ice, even grease ice, was observed only when shipboard SSTs were less than around −1.5 ℃. Accordingly, the gauge was sufficiently accurate for this discussion.

Reviewer comment R#2-23 : L212. No s after MIZ.

Author response "s" removed.

Reviewer comment R#2-24 : L218. 'forseeable'→'visible'.

Author response This section is modified and the sentence is removed. Please see author's response to R#2-5.

Reviewer comment R#2-25 : L223. 'The sea ice tends to cluster, so it appears dense where the ice exists.' - reword.

Author response Please see author's responses to R#2-5 R#2-24.

Reviewer comment R#2-26 : L230. 'depict the'→'show that the' ?

Author response Changed as suggested.

Reviewer comment R#2-27 : L264. What does 'best practice wave models' mean? Perhaps replace with 'commonly used'?

Author response Changed to "high quality". Please see the revised manuscript P8L230.

Reviewer comment R#2-28 : L266. 'a bit over' - informal language.

Author response Changed to "slightly".

Reviewer comment R#2-29 : L277. 'as uncertainty generally increased in the MIZs.' - unclear. No s after MIZ.

Author response "in the MIZs" removed as it was unnecessary. Please see the revised manuscript P8L243.

Reviewer comment R#2-30 : L299. remove the rest of the sentence after 'ongoing work' - not necessary.

Author response Removed the sentence as it was unnecessary.

Reviewer comment R#2-31 : L323. add 'that' - 'demonstrated that'.

Author response Added "that".

Reviewer comment R#2-32 : L338. 'like a'→'as a'.

Author response Changed as suggested.

Reviewer comment R#2-33 : L339. 'effects. . .are' (not is).

Author response Corrected.

Reviewer comment R#2-34 : L443. Reword.

Author response The sentence is removed as it was unnecessary.

Marked-up manuscript

The marked-up manuscript with major changes indicated by the magenta text follows the references.

References

G. Boutin, C. Lique, F. Ardhuin, C. Rousset, C. Talandier, M. Accensi, and F. Girard-Ardhuin. Toward a coupled model to investigate wave-sea ice interactions in the arctic marginal ice zone. *The Cryosphere Discussions*, 2019:1–39, 2019. https://doi.org/10.5194/tc-2019-92.

Josefino C. Comiso, Walter N. Meier, and Robert Gersten. Variability and trends in the Arctic sea ice cover: Results from different techniques. *Journal of Geophysical Research: Oceans*, 122(8): 6883–6900, 2017. https://doi.org/10.1002/2017JC012768.

N. Ivanova, L. T. Pedersen, R. T. Tonboe, S. Kern, G. Heygster, T. Lavergne, A. Sørensen, R. Saldo, G. Dybkjær, L. Brucker, and M. Shokr. Inter-comparison and evaluation of sea ice algorithms: towards further identification of challenges and optimal approach using passive microwave observations. *The Cryosphere*, 9(5):1797–1817, 2015. https://doi.org/10.5194/tc-9-1797-2015.

A.L. Kohout, M.J.M. Williams, T. Toyota, J. Lieser, and J. Hutchings. In situ observations of wave-induced sea ice breakup. *Deep Sea Research Part II: Topical Studies in Oceanography*, 131:22 – 27, 2016. ISSN 0967-0645. https://doi.org/10.1016/j.dsr2.2015.06.010.

Graig Sutherland, Jean Rabault, Kai H. Christensen, and Atle Jensen. A two layer model for wave dissipation in sea ice. *Applied Ocean Research*, 88:111 – 118, 2019. https://doi.org/10.1016/j.apor.2019.03.023.

Satellite retrieved sea ice concentration uncertainty and its effect on modelling wave evolution in marginal ice zones

Takehiko Nose[1], Takuji Waseda[1], Tsubasa Kodaira[1], and Jun Inoue[2]

[1]Graduate School of Frontier Sciences, The University of Tokyo, Kashiwa, Japan
[2]National Institute of Polar Research, Tachikawa, Japan

Correspondence: Takehiko Nose (tak.nose@k.u-tokyo.ac.jp)

Abstract. Ocean waves are known to decay exponentially when they interact with sea ice. Wave-ice models implemented in a spectral wave model, e.g., WAVEWATCH III® (WW3), derive the attenuation coefficient based on several different model ice types, i.e., how the model treats sea ice. In the marginal ice zone (MIZ) with sea ice concentration (SIC) < 1, the wave attenuation is moderated by SIC: this implies that the subgrid scale physics is missing, and the accuracy of SIC plays an important role in the predictability. Satellite retrieved SIC data (or a sea ice model that assimilates them) are often used to force wave-ice models, but these data are known to have uncertainty. Six satellite retrieved SIC products, based on four algorithms applied to SSMIS and AMSR2 data, were used in the WW3 hindcast experiment to study the effect of SIC uncertainty ΔSIC on modelling MIZ waves during the 2018 R/V Mirai observational campaign in the refreezing Chukchi Sea. The results show that ΔSIC can cause wave prediction discrepancies in ice cover. There is evidence that bivariate uncertainty data (model significant wave heights and SIC forcing) are correlated, although off-ice wave growth is more complicated due to the cumulative effect of ΔSIC along an MIZ fetch. Further, we found that the effect of ΔSIC can be large enough, such that it overwhelms the choice of model ice types, i.e., wave-ice interaction parameterisations. Despite these parameterisations being derived from different concepts and missing the subgrid scale physics relating to sea ice field heterogeneity, the accuracy of satellite retrieved SIC used as model forcing is the primary error source of modelling MIZ waves in the refreezing ocean.

1 Introduction

Satellite remote sensing and in situ observations reveal the Arctic Ocean sea ice has been declining in extent and volume (Maslanik et al., 2007; Kwok and Rothrock, 2009; Stroeve et al., 2012). Stroeve and Notz (2018) highlighted the emergence of consecutive monthly negative sea ice extent anomalies in recent years. From a practical view point, this downward trend of sea ice decline opens trans-Arctic shipping routes connecting Europe and Asia for longer times of the year; potential global economic benefits of non-ice breakers accessing Northern Sea Route and North West Passage are substantial (Stephenson et al., 2013; Bekkers et al., 2018). The increasing vessel traffic implies that adequate prediction capabilities will become crucial to

assist ships in polar waters to circumnavigate hazards such as high winds and waves, collision with perennial sea ice, and sea-spray icing; however, Jung et al. (2016) describe that the existing polar prediction systems need to be urgently enhanced to effectively manage the risks and opportunities associated with growing human activities. In this regard, the Polar Prediction Project (PPP) has contributed to advancing the predictive capabilities. While wave forecasting in polar oceans is still in its early years, the need for advancing wave forecast capacity will only grow in the emerging Arctic Ocean. This paper focuses on the effect of sea ice concentration (SIC) uncertainty on third-generation spectral wave model simulations in and near a marginal ice zone (MIZ). WMO (2014) defines the MIZ as "the region of an ice cover which is affected by waves and swell penetrating into the ice from the open ocean". This study is primarily focused on the MIZ region at the interface between the open ocean and sea ice field.

Documented academic work on wave-ice interactions has a long history dating back as far as Greenhill (1886) (V.A. Squire, 2007; Mosig et al., 2015). When wind waves propagate through/under sea ice cover, the dispersion relation is modified and wave energy is attenuated due to non-conservative dissipation and a conservative scattering phenomenon. Standalone contemporary spectral wave models simulate wave-ice interactions using sea ice as forcing; in this space, the intensive field measurements of the Arctic Sea State and Boundary Layer Physics Program (Thomson et al., 2018) have made a solid contribution to the recent advance of The WAVEWATCH III® Development Group (WW3DG) (2019) wave-ice interaction parameterisations. Rogers et al. (2016); Cheng et al. (2017); Ardhuin et al. (2018); Boutin et al. (2018) describe the development and optimisation of the latest WW3 parameterisations for wave evolution in sea ice cover. Despite the progress, Squire (2018); Thomson et al. (2018) qualify accurately quantifying the wave decay and connecting the associated mechanisms over a large domain still remain a challenge because sea ice fields are notoriously heterogeneous; therefore, the wave-ice interaction parameterisation is a source of uncertainty when simulating wave evolution in MIZs. Recent developments of coupled wave-ice-ocean models on a pan-Arctic scale (Boutin et al., 2019; Roach et al., 2019; Zhang et al., 2020) reflect the growing interest in the surface waves' role in the atmosphere, ocean, and sea ice dynamics: perhaps this indicates that advancing the wave-ice interaction physics is becoming a more pertinent issue to broader scientific communities.

Besides the model interior, e.g., wave-ice interaction parameterisations, the 0^{th} order uncertainty pertains to sea ice forcing accuracy such as SIC and sea ice thickness (SIT). In particular, SIC retrieved from satellite radiometers (or sea ice models that assimilate satellite observations) forms the most fundamental input into wave-ice models and should have a profound effect on sea state predictions. Spatial distributions of SIC in the Arctic Ocean can be mapped daily based on satellite microwave radiometry, and they have been the primary source of sea ice trend and climatological studies; however, discrepancies among retrieval algorithms have been a long-known issue, and numerous intercomparison studies have investigated the effects of retrieval algorithms, and to a lesser extent instruments, on SIC estimates (Comiso et al., 1997; Meier, 2005; Andersen et al., 2007; Notz, 2014; Ivanova et al., 2015; Comiso et al., 2017; Chevallier et al., 2017; Roach et al., 2018; Lavergne et al., 2019). To date, there is no robust validation of any algorithm, so users are urged to understand strengths and weaknesses of the algorithms when using and interpreting the data (Ivanova et al., 2015; Comiso et al., 2017). The long-known SIC discrepancies imply there is uncertainty in the knowledge of true sea ice coverage (Notz, 2014). The uncertainty is potentially greater for MIZs in the refreezing ocean as satellite derived SIC estimates are known to underestimate thin ice less than 35 cm (Heygster

et al., 2014; Ivanova et al., 2015). Because the satellite retrieved SIC has uncertainty, the choice of a SIC product a modeller and model developers select is an error source. Since the latest WW3 wave-ice parameterisation developments have all used different sea ice forcing products, understanding the effect of SIC uncertainty on wave predictions is a relevant contribution and is the primary objective of this paper.

The expedition that inspired this study is introduced to close the preliminary section: the R/V Mirai Arctic Ocean observational campaign in the refreezing Chukchi Sea during November 2018 (JAMSTEC, 2018). A 12 day MIZ transect observation was conducted to capture daily changes in the sea ice field and the associated environmental conditions at the same geographical location. The observation showed firsthand how surface waves propagate through a heterogeneous MIZ sea ice field. We began to inquire how the sea ice field heterogeneity may affect a wave-ice model and how the satellite retrieved SIC represents the observed sea ice field, which led to the subject of satellite retrieved SIC. The ensuing Section 2 introduces the methods employed to analyse the wave model uncertainties associated with SIC forcing including the R/V Mirai observation details. Section 3 discusses the SIC from a wave modelling perspective using the snapshot images of a sea ice field obtained during the MIZ transect observation. A wave hindcast experiment is conducted using various SIC products as forcing for which the model results are compared with limited available in situ wave observations and two independent predictions as described in Section 4. The analysis is extended to the refreezing Chukchi Sea to examine the bivariate uncertainty data (model significant wave heights and SIC forcing) from a physical view point of modelling wave decay and growth, which is discussed in Section 5. In this section, we also investigate the relative significance of the SIC uncertainty compared with the wave-ice interaction parameterisation uncertainty. Section 6 concludes and discusses the study findings.

2 Methods

2.1 R/V Mirai and drifting buoy observations

R/V Mirai MIZ transect observation

Regions in the Arctic Ocean, like the Chukchi Sea, that were inaccessible in November are now open for navigation, even for non-icebreakers, and R/V Mirai, a Japanese ice class vessel (JAMSTEC, 2019), carried out a late autumn voyage in 2018. R/V Mirai arrived in the Chukchi Sea on 4 November; after other ship time commitments, it began a 12 day transect observation that included an MIZ during daylight hours on 9 November. Daylight hours are limited at high latitudes during this time of the year, so sea ice observation was conducted generally between 19:00–00:00 UTC each day. The transect spanned roughly from 73.00° N, 198.00° E in the MIZ to 72.00° N, 194.00° E towards the central Chukchi Sea. Although the MIZ coverage was less expansive, daily observation of the sea ice conditions at the same geographical locations for an extended period is rare if not unique because of exhaustive ship time required. The R/V Mirai transect on 15 November is overlaid on the mosaic of Sentinel-1 A and B Synthetic Aperture Radar (SAR) normalised radar cross section (NRCS) images (NOAA, 2019) captured on the same day in Figure 1. Shipboard measurements used in this study include surface wind, sea surface temperature (SST),

air temperature, and surface wind waves (WM-2 and Piper-C#15). The details of the R/V Mirai measurement systems are provided in Appendix A.

Drifting buoy wave measurement

Two drifting type wave buoys were also deployed during the R/V Mirai observational campaign. One failed within hours, but the other buoy, Piper#13, survived for 19 days after being deployed on 6 November 2018 22:18; it was remotely switched to a sleep mode to preserve battery on 26 November, and the remote connection ceased on 5 December for some unknown reason. Hardware and on-board data processing were mostly the same as Nose et al. (2018) except Piper#13 produced bulk parameters at 15 minute intervals, which were transmitted near real time via Iridium satellite communication. Piper#13 was deployed at 73.32° N, 201.09° E, and its track between 6 and 27 November is presented in Figure 1 overlaid on the NRCS mosaic. The wave height is calculated as $H_{m0} = 4\sqrt{m_0}$ within the analysed range of a spectrum between the low and high cut-off frequencies, *f*_low and *f*_high, respectively. $m_0 = \int_{f\_\mathrm{low}}^{f\_\mathrm{high}} S(f)df$ where S is the variance density spectrum.

2.2 Satellite retrieved sea ice concentration

SIC estimates from Earth-orbiting satellites are an indirect measurement calculated from microwave brightness temperatures. Although passive microwave radiation has low energy, brightness temperatures between sea ice and open ocean are distinguishable due to the difference in surface emissivity and physical temperatures. Microwave brightness temperatures measured from different frequency channels can account for the spatial and temporal variations of the ocean surface, so retrieval algorithms can be applied to produce SIC field estimates (Comiso et al., 2017).

Since the 1970's, a number of multichannel passive microwave radiometers have been in operation, and the sensors currently in operation (that are most used) for sea ice analysis are SSMIS and AMSR2. The key difference between the two sensors to derive the SIC spatial distribution is footprint resolution as the latter instrument has around 3–4 times higher resolutions for frequencies near 19, 37, and 89 GHz. For these two sensors, a large number of SIC retrieval algorithms have been developed primarily because different algorithms produce considerably different SIC estimates. This is evidenced by a long list of intercomparison studies (Comiso et al., 1997; Meier, 2005; Andersen et al., 2007; Notz, 2014; Ivanova et al., 2015; Comiso et al., 2017; Chevallier et al., 2017; Roach et al., 2018; Lavergne et al., 2019).

A total of eight SIC products were selected for this uncertainty study based on four algorithms applied to SSMIS and AMSR2 data. Hereinafter, uncertainty of satellite derived SIC c_i for a set of data products is defined as follows:

$$\Delta c_i = uncertainty(c_i) = max(c_{i1}, ..., c_{i8}) - min(c_{i1}, ..., c_{i8}) \quad (1)$$

where c_{ix} is the respective data products. Four algorithms that appear most frequently in literature were considered, and the following algorithms were selected: NASA-Team (Cavalieri et al., 1984), Bootstrap (Comiso, 1986), OSISAF, and ARTIST-sea-ice (Spreen et al., 2008). The selected products are summarised in Table 1 where the product abbreviations and data references are also provided.

A concise explanation for the selection of each product is given below:

– NASA-Team—the algorithm has been used for sea ice trend and climatological studies since the beginning of the satellite radiometry era. The SIC data used in this study are the original NASA-Team algorithm applied to SSMIS data and the enhanced NASA-Team2 algorithm applied to AMSR2 data.

– Bootstrap—like NASA-Team, the Bootstrap algorithm has been used for sea ice trend and climatological studies for many years. The SIC data used in this study are the Bootstrap algorithm applied to SSMIS and AMSR2 data.

– OSISAF—this algorithm was selected because the highly reputable European Centre for Medium-Range Weather Forecasts (ECMWF) wave model (ECWAM) uses sea ice forcing based on the Operational Sea Surface Temperature and Sea Ice Analysis (OSTIA) system (Donlon et al., 2012) for which SIC is retrieved using the OSISAF algorithm applied to SSMIS data. We also analyse the AMSR2 data in this study.

– ARTIST-Sea-Ice—this algorithm uses the 89 GHz frequency signal to produce high resolution SIC estimates. This algorithm was selected as accurate higher resolution forcing is generally desirable for numerical models. For this product, we only use the AMSR2 data but analyse two different grids: the pan-Arctic data with 6.250 km resolution and the regional Chukchi-Beaufort data with 3.125 km grid resolution.

The principle of all sea ice algorithms as described in Comiso (2007) is that measured radiative flux can be expressed as $T = T_i c_i + T_o c_o$ where T_i and T_o are the brightness temperatures normally observed from 100 % ice cover and 100 % open water, respectively. Then, SIC can be expressed simply as $c_i = \frac{T_b - T_o}{T_i - T_o}$ where the subscript b corresponds to observed ocean surface, and the ice-free surface is $c_o = 1 - c_i$ (Comiso, 2007). The accuracy of SIC is then dependent on the closeness of tuning brightness temperature tie points to the ice-free and fully ice-covered ocean surface. The selection of frequency channels to derive polarisation ratios or differences (V and H) and gradient ratios (V polarisation) to retrieve SIC also dictates strengths and uncertainties of each algorithm. Technical details of the respective algorithms are described in the Table 1 data references.

2.3 WAVEWATCH III ® spectral wave model

The effect of SIC uncertainty on MIZ wave predictions was investigated by a hindcast experiment using The Arctic Ocean wave model developed at the University of Tokyo (TodaiWW3-ArCS) based on WW3, which was introduced in Nose et al. (2018). Third-generation spectral wave models simulate the numerical evolution of waves as energy budgets based on the action density balance equation,

$$\frac{\partial N}{\partial t} + \nabla \cdot \boldsymbol{c} N = \frac{s}{\sigma}. \tag{2}$$

The left hand side concerns wave kinematics where N is the wave action density spectrum, which is a function of frequency σ, direction θ, x and y space, and time t, and $\boldsymbol{c}$ describes the propagation velocities in spatial and spectral coordinates. In deep water when neglecting currents, $\boldsymbol{c}$ is the group velocity $\boldsymbol{c}_g$. Source terms are on the right hand side and the ones relevant to this study include the following: the wind input term s_{wind}, the wave dissipation term $s_{\text{dissipation}}$, the non-linear interaction term $s_{\text{non-linear interactions}}$, and the wave-ice interaction term s_{ice}. The sum of these source terms s is expressed based on the following

default scaling in ice-covered waters:

$$s = (1 - c_i)(s_{\text{wind}} + s_{\text{dissipation}}) + c_i s_{\text{ice}} + s_{\text{non-linear interactions}}. \quad (3)$$

Specifically to this study, c_i relates to the satellite retrieved SIC and s_{ice} to the ice type, i.e., how the model treats sea ice. The effect of sea ice on waves are represented via the modified dispersion relation $\sigma = \sigma(\overline{k})$ where $|\overline{k}| = k = k_r + ik_i$. The real part k_r is the physical wavenumber and alters the propagation speed of waves in a sea ice field (analogous to effects of shoaling and refraction by bathymetry), and the imaginary part k_i is the exponential decay coefficient. k_i is introduced in the model as $s_{\text{ice}} = -2c_g k_i N$ for fully ice-covered sea, i.e., c_i=1, and the solution to $\frac{dN}{dt} = s_{\text{ice}}$ is $N_0 e^{-2c_g k_i t}$. There are five options for treating sea ice in WW3 denoted as IC1–5; c_i provides the scaling in the linkage between s_{ice} and ICX as

$$\frac{dN}{dt} = c_i s_{\text{ice}} = -2c_i c_g k_i(f, p_1, ..., p_n)N \quad (4)$$

where p_n is the sea ice properties, e.g., effective shear modulus and effective viscosity. Therefore, the rate of attenuation depends on the wave period and sea ice properties and is moderated by c_i, i.e., $N_0 e^{-2c_i c_g k_i t}$.

The wave-ice models implemented in WW3 that calculate k_r to model k_i are IC2, IC3, and IC5. IC2 calculates dissipation due to basal friction in the boundary layer below an ice sheet, which is modelled as a continuous thin elastic plate based on the work of Liu and Mollo-Christensen (1988). IC3 treats sea ice as a visco-elastic layer based on Wang and Shen (2010), which calculates the internal stress of the ice cover based on storage and dissipation. IC5 is a visco-elastic beam model based on Mosig et al. (2015). The dispersion relation of these models are provided in Appendix B. Ardhuin et al. (2018); Boutin et al. (2018) (IC2) and Rogers et al. (2016); Cheng et al. (2017) (IC3) describe the progress of these s_{ice} parameterisations using the refreezing Beaufort Sea data of Thomson et al. (2018). These wave-ice models can be combined with an energy-conservative scattering attenuation model denoted as IS1 and IS2 (Meylan and Masson, 2006; Dumont et al., 2011; Williams et al., 2013; Ardhuin et al., 2018; Boutin et al., 2018).

During the R/V Mirai cruise, sea ice in the MIZ was mainly grease, nilas, and pancake ice, so the hindcast experiment was conducted using the IC3 package (with the default parameters) as it has been designed for these ice types (Rogers et al., 2016; Cheng et al., 2017). Scattering is not expected to be the dominant process in this type of ice fields (Montiel et al., 2018), so it was not considered in the experiment. Regarding SIT forcing, a homogeneous input option with a value of 10 cm was applied; the constant forcing was applied so we can evaluate solely the Δc_i effect on wave-ice interaction models. 10 cm was chosen because the MIZ transect observation was mostly characterised by new and young ice whose upper bound of SIT is of a similar order (Canadian Ice Service-Environment Canada, 2005).

s_{wind} and $s_{\text{dissipation}}$ parameterisations and wind forcing for TodaiWW3-ArCS were tested. We compared the most commonly used physics packages, ST4 (Ardhuin et al., 2010; Rascle and Ardhuin, 2013) and ST6 (Rogers et al., 2012; Zieger et al., 2015; Liu et al., 2019), using ECMWF global reanalysis (ERA5) 10 m wind (U_{10}) against the 2016 September storm (Nose et al., 2018) when TodaiWW3-ArCS and observations agreed well. The ST6 parameterisation showed marginally improved agreement using the default parameters; so all simulations used the ST6 parameterisation and were forced with ERA5 wind fields. The default $s_{\text{non-linear interactions}}$, which is not affected numerically by sea ice, was used for all simulations.

TodaiWW3-ArCS used in this study has a horizontal resolution of 4 km, and its domain covers most of the Pacific side of the Arctic Ocean including the East Siberian, Chukchi, and Beaufort Seas. The model boundaries connected to the seas of the Arctic Ocean was enclosed by ice cover during the November 2018 modelling period (corresponding to the R/V Mirai observation), so nesting was unnecessary. Similar to Rogers et al. (2016), we neglected swell penetration through the Bering Strait. The technical details of TodaiWW3-ArCS's geographical and spectral grids are provided in Appendix B.

ASI-3km and OSISAF-AMSR2 data were excluded for the wave hindcast experiment. The former has a regional coverage that is too small for the TodaiWW3-ArCS domain, and the OSISAF-AMSR2 data have noise in the open ocean, which yield erroneous wave simulation results when they are used as model forcing (as described in Appendix C). The remaining six satellite retrieved SIC products in Table 1 were used as model forcing to examine wave modelling uncertainty, so the Δc_i wave hindcast experiment dataset has $\{H_{m0\,\mathrm{c_i}1}, ..., H_{m0\,\mathrm{c_i}6}\}$ where c_{ix} denotes the satellite retrieved SIC forcing. Step-like changes of SIC from daily intervals are not ideal as forcing, so the SIC data were interpolated to match the model output frequency of hourly intervals. Unless specified otherwise, all other settings were default. The modelling period covers both R/V Mirai and Piper#13 observations and is from 5 to 25 November 2018 with a 5 day spin up.

It should be noted that when satellite derived SIC data are used as forcing, the heat and momentum fluxes are distorted in the marine atmospheric boundary layer because the lower atmosphere and the ocean surface are no longer coupled. Inoue et al. (2011) evaluated surface heat transfer from three reanalysis products by focusing on how the models treat sea ice; they found the treatment of SIC is a key factor for the estimation of surface turbulent heat fluxes. Guest et al. (2018) have elucidated the ice-edge jet generation mechanism based on the in situ data obtained in the refreezing Beaufort Sea. Undoubtedly, altering the sea ice field would feedback to the wind, but this is not captured in this wave hindcast experiment.

3 Sea ice concentration: definition, characteristics, and the use in wave-ice models

WMO (2014) defines SIC as "the ratio expressed in tenths describing the amount of the sea surface covered by ice as a fraction of the whole area being considered". The so-called "area considered" presumably varies for different objectives. The length scale of $O(10)$ km may be adequate for sea ice extent climatology, but for wave-ice interactions, the wave provides a scale in a phase-resolved sense. Satellite retrieved SIC represents the fraction of ice-covered water over a large area, sufficiently large enough that the SIC represents a property of a continuum. In reality, the sea ice in the MIZ is granular, and ice floes jam due to horizontal convergence by Langmuir circulation, internal waves, and wind variability, resulting in a formation of features such as ice bands and wind streaks—with which waves likely interact distinctively.

On 14 November 2018 during the MIZ transect observation, R/V Mirai encountered moderate on-ice waves with an H_{m0} up to around 2.00 m propagating towards the ice edge (this H_{m0} estimate is consistent from both the shipboard wave data described in Appendix A and hindcast models as shown later). Figure 2 presents a series of snapshot images of the sea ice field during the encounter. R/V Mirai traversed over 10 km in the MIZ from the ice edge, and each image area extends at least over 1 km conservatively (using the crude distance to horizon calculation). These images depict the heterogeneous sea ice field, both in SIC and ice types, that waves propagate when they enter an MIZ. Because WW3 wave-ice interaction models are

scaled according to $\frac{dN}{dt} = c_i s_{\text{ice}}$ (Equation 4), the subgrid scale physics is completely missing. It is plausible the subgrid scale distribution of SIC and ice types can be treated in a stochastic manner to provide meaningful mean values to the grid-scale model. On the other hand, SIC c_i also affects the WW3 wave-ice model by means of scaling (Equation 4). Figure 2 shows SIC data from eight satellite retrieved products described in Section 2.2 during this event. The SIC estimates interpolated at the R/V Mirai positions largely deviate among the products, characterising the uncertainty of the satellite retrieved SIC. Moreover, the entire time series of the 12 day MIZ transect observation depicts Δc_i is persistent (Figures A4 to A6 of Appendix D). Hereafter, we show how large the effect of Δc_i on modelling MIZ waves can be, so much so that it overwhelms the choice of s_{ice}, e.g., ICX.

4 Δc_i effects on wave modelling at the observation sites

Our goal is to understand Δc_i effects on wave-ice models, but adequate model accuracy, at least qualitatively, is needed for a meaningful uncertainty analysis. Because we lack a sufficient duration of robust in situ wave measurements, two independent numerical wave models that produce predictions in the Arctic Ocean, namely ERA5 ECWAM and the Arctic Monitoring and Forecasting Centre (ARCMFC) wave model, both based on WAM, were also included in the analysis. Comparisons with these high quality models provide a guide on the TodaiWW3-ArCS performance. The ERA5 ECWAM data are made available on a 0.5° resolution grid on the Climate Data Store (Copernicus, 2019), and the model treats grid points with $c_i > 0.30$ as land using an ice mask. The ARCMFC wave model has a horizontal resolution of around 8 km and also used an ice mask; from December 2019, the month after our observation, the model was upgraded to simulate waves under sea ice cover based on Sutherland et al. (2019)'s two-layer sea ice model. The ARCMFC TOPAZ model provides the SIC and SIT forcing fields, which are kept constant from the initial state. Daily ARCMFC wave analysis data remapped to a 6.25 km polar stereographic grid are made available on ARCMFC (2019).

R/V Mirai MIZ transect observation

Figure 3 presents time series of H_{m0} interpolated at the R/V Mirai positions for all models during the MIZ transect observation (refer to Appendix D for the details on the environmental conditions during the MIZ transect observation). The figure also includes shipboard wave measurements from the WM-2 integrated analog system (TSK Tsurumi Seiki Co., 2019) when the ship speed was < 2 ms^{-1} (refer to Appendix A for further explanation). Using Equation 1, the model wave height uncertainty is denoted $\Delta H_{m0} = uncertainty(H_{m0})$ for six SIC forcing simulations. The time series figure depicts the effect of sea ice on waves each time R/V Mirai sailed in the ice cover as the uncertainty generally increased. In the case of waves propagating towards the ice edge, waves decay at different timing depending on the sea ice edge location of the respective SIC data used, and the representation of the ice edge affects the fetch distance of off-ice wave growth as waves propagate towards open water. The model $\Delta H_{m0} > 1.50$ m occurred on 20 November 2018 during the off-ice wind condition, which is > 50 % of the open water H_{m0} (of the TodaiWW3-ArCS and ARCMFC models). Because R/V Mirai slowed down in the MIZs, at least one WM-2 measurement was obtained in ice cover each day, and they generally lie within $[min(H_{m0\,\mathrm{c_i}1}, ..., H_{m0\,\mathrm{c_i}6}), max(H_{m0\,\mathrm{c_i}1}, ..., H_{m0\,\mathrm{c_i}})]$.

Furthermore, when the open ocean sea state is energetic, daily peak ΔH_{m0} occurs as R/V Mirai sailed into and out of the ice-covered water, indicating the representation of an ice edge in the model forcing plays an important role.

Regarding the comparison of three different base models, ERA5 ECWAM consistently has a positive bias compared with other models except for the on-ice wave event on 14 November when they all agree reasonably well. For this event, both WM-2 and Piper-C#15 have comparable estimates of the measured peak H_{m0} as R/V Mirai was sailing out of the ice cover, which was around 2.00 m. The ERA5 ECWAM positive bias compared with other models is exacerbated when the strongest off-ice winds were recorded by R/V Mirai between 19–22 November. ARCMFC H_{m0} agrees slightly better with $max(\text{TodaiWW3-ArCS}H_{m0})$. These are evidenced in bias and root mean square deviation (RMSD) values calculated with respect to the ARCMFC H_{m0}: the ERA5 ECWAM H_{m0} has bias = 0.19 m and RMSD = 0.25 m, and the $max(\text{TodaiWW3-ArCS}H_{m0})$ has bias = −0.11 m and RMSD = 0.21 m.

It is interesting to point out that using different sea ice forcing alone causes wave estimates to deviate in open water. This is also the case between the ERA5 ECWAM and ARCMFC models, which both use ECMWF wind forcing. The deviation of wave estimates in open ocean is more apparent during the off-ice wind conditions at the end of the transect observation period. A conjecture is that a different treatment of sea ice in each model modifies available fetch for which waves can be generated; for example, having open water to 0.30 SIC in ERA5 ECWAM may simply increase the fetch distance at the R/V Mirai locations, which could result in a consistent positive bias compared with other models.

Piper#13 drifting buoy observation

Figure 4 is a Piper#13 equivalent of Figure 3 with its observational data. Satellite retrieved SIC for all products at the Piper#13 positions is provided in Figure A7 of Appendix D. The buoy data are discussed first. It measured $H_{m0} > 1.00$ m for two days after being deployed at the finals hours on 6 November 2018. H_{m0} tapered off to around 0.20 m, but briefly rose to 0.60 m when the wind speed increased at around 12 November 2018 00:00. Then, it drifted in ice cover with less wave penetration; no measurable wave signals propagated to Piper#13 as the measured spectra indicate instrument noise except during the on-ice wave event between the late hours on 14 November and the early hours of 15 November. Peak wave periods, T_p, which is a frequency inverse corresponding to the maximum variance density, were consistently around 9 s; this is likely a true wave signal even though H_{m0} was only 0.05 m.

Regarding the wave hindcast, TodaiWW3-ArCS ΔH_{m0} was the largest in open water and decreased with $mean(H_{m0})$. In general, Piper#13 H_{m0} during 7 and 8 November are underestimated by all numerical models. When the wave energy tapered off between 8–11 November, both ERA5 ECWAM and ARCMFC model H_{m0} are overestimated. However, the episodic increase of wave energy on 11 and 12 November is reproduced in these models, albeit with a positive bias, whereas the TodaiWW3-ArCS simulations did not show any increase in the H_{m0} at the Piper#13 location. There are no data shown for the ERA5 ECWAM and ARCMFC models after 12 November at Piper#13 presumably due to the ice masks. There are three occasions when all TodaiWW3-ArCS simulations slightly overestimates H_{m0} compared with the buoy data, which indicate the model attenuation rates may be too weak or SIC forcing is inaccurate.

5 Δc_i and wave modelling in the refreezing Chukchi Sea

Figure 5 depicts 0.15 and 0.85 SIC contours on 15 November 2018 from three products: OSISAF-SSMIS, BST-AMSR2, and ASI-3km. They are overlaid on the NRCS mosaic of Sentinel-1 images acquired on the same day as NRCSs provide indication of true sea ice fields. The difference among these contours in the MIZs is striking regardless of their footprint resolutions. The mosaic depicts sea ice edges have a wavy, but highly nonlinear, jagged form. For most of the ice edges, Figure 5 shows OSISAF-SSMIS derived 0.15 contours are smoother whereas the BST-AMSR2 and ASI-3km contours appear to follow the sea ice edge concavity and convexity with a varying degree of closeness; ASI-3km appears to be qualitatively more consistent with the ice edges detected in the NRCS data. Figure 5 also shows the 0.85 SIC contours are somewhat qualitatively similar between OSISAF-SSMIS and ASI-3km; however, BST-AMSR2 and OSISAF-SSMIS 0.85 contours can be some 200 km apart, for example between 73.00° N, 190.00° E and 74.00° N, 185.00° E. Regions of low radar intensity that appears dark in the NRCSs are apparent in the disparate 0.85 SIC contours, which indicate the waters in this area were not high SIC. As such, it does imply BST-AMSR2 overestimated the SIC for this date. Although not shown here, 0.50 SIC contours are inconsistent among all three products. The analysis here suggests ASI-3km generally captures qualitatively the SIC spatial variability shown in the NRCS data.

The above suggests the satellite retrieved SIC uncertainty can be considerable on a regional scale. The preceding Section 4 demonstrated that simply changing SIC forcing alone produces considerable ΔH_{m0} in the wave hindcast experiment at the observation sites. In this section, we extend the wave hindcast analysis to the refreezing Chukchi Sea.

5.1 On- and off-ice wave evolution in the refreezing Chukchi Sea MIZs

A more in-depth analysis is conducted here to understand how Δc_i affects the wave-ice interactions as implemented in WW3 from a physical view point. At the most fundamental level, sea ice fields modify the fetch of the ocean: two cases are selected to analyse the effect of varying fetches on the attenuation and growth during on- and off-ice wave conditions on 15 November 2018 00:00 and 21 November 2018 18:00, respectively. The wind magnitudes and vectors for these cases are shown in Figure 6. For the on-ice wave case, relatively strong small-scale south westerly winds as depicted in Figure 6a generated waves with an H_{m0} of about 2.00 m propagating towards the ice edge. When on-ice waves encounter ice cover, rapid attenuation is expected within $O(10)$ km (Ardhuin et al., 2018; Squire, 2018), so the ice edge locations and the SIC variability near it affect the model simulation of wave decay. For the selected off-ice wave case, a low pressure system over Alaska and a high pressure system north west of the Chukchi Sea generated sustained north easterly winds over much of the Chukchi Sea as depicted in Figure 6b, which generated open water $H_{m0} > 3.00$ m. In this case, the ice edge and SIC field determine the fetch on which waves are generated, and as such, Δc_i introduces ΔH_{m0}.

Owing to the combination of the non-homogeneous nature of wind that generates waves and the SIC field heterogeneity, there was no statistical association for the bivariate uncertainty data (ΔH_{m0} and Δc_i) even when the H_{m0} was normalised to wind forcing. In an attempt to elucidate the model uncertainties in the context of physical processes, a scatter plot is produced for both cases with the following visualisation technique: marker sizes are scaled to $mean(H_{m0})$ as a bubble plot and each marker is colour coded according to $mean(c_i)$ like a colour-coded scatter plot. The former aims to emphasise the model data

near the ice edge where the effects of wave attenuation and growth associated with Δc_i are most prominent, and the colour coded markers indicate $mean(c_i)$ among all forcing. For simplicity, we refer to these figures herein as an enhanced scatter plot.

Figure 7a depicts the spatial distribution of the model ΔH_{m0} for the on-ice wave case with 0.01, 0.50, and 0.85 $mean(c_i)$ contours. Not all ice edges are aligned to the on-ice wind orientation because of the ice edge geometry. On-ice wave analysis was, therefore, conducted for a strip of the model grid points roughly 100 km in width along the south westerly on-ice wind orientation as depicted in a grey dashed quadrilateral. An enhanced scatter plot shown in Figure 7b depicts bivariate uncertainty data corresponding to the model grid points along the on-ice wind orientation. There is a strong indication of a correlation between the Δc_i and model ΔH_{m0} for this on-ice wave case. The correlated uncertainties imply that as on-ice waves approach and decay due to wave-ice interactions, larger discrepancies in the representation of SIC as forcing causes greater model ΔH_{m0}.

Figure 7b also shows inverse proportion of marker sizes and uncertainties. Smaller size markers have low $mean(H_{m0})$, so larger ΔH_{m0} occur when only one or two of $\{H_{m0\,c_i1}, ...H_{m0\,c_i6}\}$ have $H_{m0} > 0$ while remaining $H_{m0} = 0$ due to waves being fully attenuated. The figure shows only blue and light-blue markers, which indicate the waves generated by the strong localised winds decayed with limited wave penetration no farther than $mean(c_i) = 0.40$. Furthermore, in theory, the cluster of data must approach the origin of the figure coordinate in the upwind open waters in the central Chukchi Sea. In other words, on-ice waves that are being generated numerically in the open water must satisfy $\Delta H_{m0} = 0$ & $\Delta c_i = 0$. The reason they do not converge to the figure coordinate origin is that the Δc_i along the Siberian coast (not shown here) affects the waves in the upwind waters as indicated by very faint yellow shades in Figure 7a.

Analysis of the off-ice case is carried out in a similar manner. The data bound by Quadrilateral 2 as shown in Figure 8a reflect the model grid points with the north easterly off-ice wind conditions. Although the correlation is not as high as the on-ice wave case (with higher scatter for $\Delta c_i > 0.10$), the enhanced scatter plot in Figure 8c shows that the bivariate uncertainty data are correlated for the off-ice wave case as well. Analogous to the on-ice wave case, high ΔH_{m0} can occur near the ice edge when only one or two simulations have the SIC forcing representing open water conditions, while the wave growth is suppressed for the remaining simulations due to higher SIC. This effect is depicted in Figure 9c, which shows ΔH_{m0} and Δc_i along a transect of the Quadrilateral 2 long axis. Along this transect, ASI-6km and BST-AMSR2 have the most north east ice edge, and the waves rapidly grow under the strong north easterly wind forcing whereas the higher SIC of the other simulations suppress the wave growth. A distinct difference between the off- and on-ice wave cases regarding the Δc_i effect on wave-ice models is that ΔH_{m0} remains in the downwind open ocean whereas $\Delta c_i \to 0$. This is clearly shown in Figure 8c where $\Delta H_{m0} = [0.10, 0.60]$ when $\Delta c_i = 0$ indicating the effect of Δc_i forcing on model ΔH_{m0} can extend to the adjacent open water.

Off-ice wave evolution is a complex process because the fetch is not only controlled by the location of the ice edge, but also wave-ice interactions as implemented in WW3. The current numerical approach to simulate wind pumping energy into waves in ice cover is dictated by c_i because waves grow when $(1 - c_i)(s_{\text{wind}} + s_{\text{dissipation}}) > c_i s_{\text{ice}}$. Whether wave evolution in ice cover follows the Equation 3 scaling has been discussed in Rogers et al. (2016); Thomson et al. (2018); the latter cites Li et al. (2017) who confirmed wind input to high frequency wave energy in the Antarctic Ocean. The off-ice ΔH_{m0} is apparently also

influenced by the cumulative effect of the Δc_i along the fetch distance affected by the wave-ice interaction parameterisations as implemented in WW3.

Lastly, for both on- and off-ice wave cases, significant ΔH_{m0} extends to the waters where the wind forcing is orientated along the ice edge; so the model data are briefly examined in the region of MIZs north east of Wrangel Island, which is shown as Quadrilateral 1 in Figure 8a along the sea ice edge and north easterly wind forcing orientation. This region has considerable Δc_i (not shown here) in a similar manner to Figure 5, and the model ΔH_{m0} is just as sizeable under the influence of high wind forcing. There is evidence of correlated bivariate uncertainty data in Figure 8b, and a combination of on- and off-ice wave features for the respective enhanced plots discussed in the previous paragraphs are apparent. Deciphering the physical processes is complicated; however, the bivariate uncertainty data along a transect illustrates how Δc_i and ΔH_{m0} are related; Figure 9b shows these results for a cross section oriented along the ice edge (the long axis of Quadrilateral 2) on 21 November 2018 18:00.

5.2 Relative significance of Δc_i compared with wave-ice interaction parameterisation uncertainty

The Δc_i hindcast experiment conducted in this study intentionally adopted the default IC3 source term parameters. As mentioned in Section 1, considerable progress in the WW3 wave-ice interaction parameterisations has been made owing to the Thomson et al. (2018) measurements. However, Ardhuin et al. (2018) also explain that observation of wave attenuation could also be reproduced with many model forcing and parameter combinations, which as stated in the article is not unexpected because different wave-ice interaction processes are taking place along the wave propagation path. As discussed in Section 2.3, WW3 offers three physics-based s_{ice} parameterisations: IC2, IC3, and IC5. They are based on different attenuation mechanisms and dispersion relations (see Appendix B), but their default ice rheological parameters (as given in the manual or the WW3 regression test cases) also vary as apparently the sea ice parameters are context-based according to the manual. The three main parameters used to tune the IC2, IC3, and IC5 attenuation rate are as follows: eddy viscosity (m^2s^{-1}) ν, ice density (kg^2m^{-3}) ρ, and effective elastic shear modulus (Pa) G, although G is not used in IC2. The default ρ values are consistent for these s_{ice} parameterisations. The default ν values are 153.6e−3, 1.0e+0, and 5.0e+7 for IC2, IC3, and IC5, respectively, and the default G values are 1.0e+3 and 4.9e+12 for IC3 and IC5, respectively. Rogers et al. (2016) adopted $G = 0$ assuming it is negligible in nilas and pancake ice fields. Based on the enormous range of tunable parameters and other factors described in this paragraph, the s_{ice} parameterisation is a notable uncertainty source. To evaluate the relative significance of Δc_i, we compared the results with the wave-ice interaction source term uncertainty (s_{ice} uncertainty) for the modelling period between 5 and 25 November 2018. The s_{ice} uncertainty wave hindcast experiment was conducted using IC2, IC3, and IC5 based on the same model setup described in Section 2.3 except all three simulations used BST-AMSR2 as SIC forcing.

A pair of ΔH_{m0} datasets were derived for the Δc_i and s_{ice} uncertainty wave hindcast experiments. They were collated for the entire simulation period within the model domain shown in Figure 7a. Uncertainty distributions are visualised in a Q-Q plot by simply sorting each dataset, and this is shown in Figure 10. The figure depicts that both uncertainties are considerable with $max(\Delta H_{m0})$ values of 1.95 m and 1.44 m for the Δc_i and s_{ice} uncertainty experiments, respectively. The robustness of this result was examined via SIT forcing sensitivity analysis. From a physical view point, the choice of 10 cm was made to match

the observed sea ice types during the R/V Mirai MIZ transect observation. For observational evidence of SIT in the refreezing Arctic Ocean, we defer to Ardhuin et al. (2018) to determine the test case and selected 50 cm. From a wave-ice modelling perspective, SIT effectively serves as a tuning parameter when forced as a homogeneous field. For example, the attenuation rate k_i of IC2 as shown in Appendix B has SIT in the form of $(1 + k_r M)$ in the denominator: $M = \frac{\rho h_i}{\rho_w}$ (Liu and Mollo-Christensen, 1988) where h_i is the SIT, and ρ and ρ_w are the ice and sea water density. If we take a deep water wavelength corresponding to 7 s wave period, changing the SIT from 10 cm to 50 cm increase the k_i by at most 3 %. k_i sensitivity on SIT examined in Wang and Shen (2010); Mosig et al. (2015) (IC3 and IC5) appears more sensitive; as such, sensitivity analysis was conducted for our model. Repeating the Δc_i and s_{ice} uncertainty experiments with 50 cm SIT, $max(\Delta H_{m0})$ values increased respectively to 2.34 m and 1.95 m, but the Δc_i remains as the dominant error source. Further, IC3 was most affected by the SIT change for the equivalent transects of Figure 9 (not shown here). Even though there was no event during the study period when scattering were expected to be the dominant process (the implication of this is given in Section 6), sensitivity of the finding to scattering was also examined by combining IS2 scattering with IC2 and IC3 with the default parameters. The results remained robust for the study period. Lastly, sensitivity to the choice of SIC forcing used in the s_{ice} uncertainty experiment was examined by using ASI-6km instead of BST-AMSR2: the experiment also resulted in the same outcome.

Table 2 is a list of SIC forcing used in the recent WW3 s_{ice} developments as well as the forcing of the wave models analysed in Section 4. Some studies employed numerical sea ice models or considered various sources and assessed their accuracy/suitability. It is interesting to learn that each wave-ice modelling study used different satellite retrieved SIC data.

6 Conclusions and discussions

The WW3 wave-ice models represent the exponential decay of waves in the presence of sea ice as $\frac{dN}{dt} = -2c_i c_g k_i N$ (Equation 4). We investigated the effect of the satellite retrieved SIC uncertainty Δc_i on modelling waves in the refreezing Chukchi Sea MIZ using six SIC data sets based on the four commonly used retrieval algorithms: NASA-Team, Bootstrap, OSISAF, and ARTIST-sea-ice. The wave hindcast experiment reveals Δc_i causes model wave height uncertainty ΔH_{m0}, and there is evidence that bivariate uncertainty data (ΔH_{m0} and Δc_i) are correlated, although off-ice wave growth is more complicated due to the cumulative effect of Δc_i along an MIZ fetch.

We compared the ΔH_{m0} distribution of the Δc_i experiment with that of the s_{ice} uncertainty experiment. Both uncertainties are found to be considerable during the simulation period with maximum ΔH_{m0} values of 1.95 m and 1.44 m, respectively. This result is found to be robust based on the sensitivity analyses that tested the SIT forcing and the inclusion of scattering. Despite the s_{ice} parameterisations being derived from different concepts and the WW3 wave-ice models completely missing the subgrid scale physics relating to sea ice field heterogeneity, the accuracy of satellite retrieved SIC used as model forcing is the primary error source of modelling MIZ waves in the refreezing ocean. The study outcome suggests wave-ice model tuning may not be as effective at this time when the knowledge of the true SIC field is too uncertain. It is worthy to note that swell waves that propagate $O(100)$ km into the ice-covered water where the scattering would likely be the dominant process were not observed during the study period. As such, the effect of Δc_i for such waves remains to be resolved.

Future improvements on the wave-ice models should come from two ends; continual developments of parameterised physics on the regional and pan-Arctic scale and working on a subgrid scale physical model on the other end. Solid and robust observational evidence through remote sensing and shipboard measurements is likely the key to connecting these two ends.

Appendix A: R/V Mirai measurement system

R/V Mirai is equipped with two anemometers that were located on the foremast at 25 m elevation, and indicative wind conditions at the ship positions were derived from 10 minute vector moving averages of 6 s interval instantaneous true wind speed and direction. SST was measured −1 m below the sea surface with further 5 m inlet to the gauge while air temperatures were measured on the foremast at 23 m elevation.

Shipboard waves were obtained based on two methods: a microwave radar system (WM-2) (TSK Tsurumi Seiki Co., 2019) at the bow and stern of the ship, and nine-axis Inertial Moment Unit (IMU) (Piper-C#15), which is a device similar to the one used by Kohout et al. (2015). WM-2 has a sampling frequency of 2 Hz and collects raw sea surface elevation for 1,152 seconds at 35 minutes past each hour, and its integrated analogue system removes hull agitation and carries out Doppler correction. Bulk parameters like the significant wave height and period are produced based on the zero-crossing method. Wave observations during the campaign from the WM-2 integrated analog system (TSK Tsurumi Seiki Co., 2019) were significantly affected by Doppler correction errors. Collins III et al. (2015) have shown shipboard measurements are less affected by this effect when ship speed is < 3 ms^{-1}. Applying a 2 ms^{-1} ship speed threshold greatly reduced conspicuously spurious data, and these data were used as indicative wave heights in this study (e.g., Figure 3). Piper-C#15 on board the vessel relies on an IMU. The processing method is consistent with Kohout et al. (2015) except 15 minute intervals were used instead of 1 hour. Waves in the Chukchi Sea during the study period was dominated by wind seas, which have shorter wavelength relative to the ship dimensions. These waves are impeded by R/V Mirai's hull, so the shipboard Piper-C#15 has limitations on measuring wind seas. Response Amplitude Operator of R/V Mirai and the WM-2 data can be combined in theory to transfer IMU's high frequency signals to true surface elevations, but post-processing remains ongoing work. Although most of the Piper-C#15 data did not reflect the true wave field, the peak Piper-C#15 H_{m0} of 2.00 m during the on-ice wave event on 14 November 2018 agreed with the peak WM-2 H_{m0}; this value is also comparable with the ERA5 H_{m0} as well. This provides confidence that the waves observed during this event was at least around 2.00 m.

Appendix B: Supplementary information of TodaiWW3-ArCS and the dispersion relation of WAVEWATCH III ® wave-ice interaction models

The TodaiWW3-ArCS geographical grid at high latitudes was based on the curvilinear grid implemented by Rogers and Campbell (2009) with a polar stereographic projection of 75° N latitude (produced by Mathworks Matlab's polarstereo_inv function). The model domain coverage on the polar stereographic grids is as follows: the easting extent between −1,800 km and 1,512 km, and the northing extent between 520 km and 2,904 km. The geographical grid was defined using the International

Bathymetry Chart of the Arctic Ocean bathymetry (Jakobsson et al., 2012) and the Global Self-consistent, Hierarchical, High-resolution Geography shoreline data (Wessel and Smith, 1996), and there are approximately 301,535 sea point cells. The spectral grid was configured with 36 directional and 35 frequency bins with the latter ranging from 0.041 Hz to 1.052 Hz.

The WW3 wave-ice model dispersion relations for IC2, IC3, and IC5 are provided here. IC2 is based on the work of Liu and Mollo-Christensen (1988), and the dispersion relation is defined as follows according to the WW3 manual:

$$\sigma^2 = \frac{gk_r + Bk_r^5}{\coth(k_r d) + (k_r M)}, \; c_g = \frac{g + (5 + 4k_r M)Bk_r^5}{2\sigma(1 + k_r M)^2}, \text{ and } k_i = \frac{\sqrt{\nu\sigma}k_r}{c_g\sqrt{2}(1 + k_r M)},$$

where

$$B = \frac{Eh_i^3}{12(1-\phi^2)\rho_w}, \; Q = \frac{Ph_i}{\rho_w}, \text{ and } M = \frac{\rho h_i}{\rho_w}.$$

h_i is the SIT, ρ and ρ_w are the ice and sea water density, ν is the viscosity, E is the Young's modulus of elasticity, ϕ is the Poisson's ratio, and P is the compressive stress in the ice pack.

IC3 is based on Wang and Shen (2010), and the dispersion relation is concisely shown in Equation 4 of Cheng et al. (2017) as follows:

$$\sigma^2 - Q_c gk\tanh(kd) = 0 \text{ where}$$

$$Q_c = 1 + \frac{\rho}{\rho_w}\frac{g^2k^2S_kC_a - (K^4 + 16k^6a^2\nu_e^4)S_kS_a - 8k^3a\nu_e^2(C_kC_a - 1)}{gk(4k^3a\nu_e^2S_kC_a + K^2S_aC_k - gkS_kS_a)},$$

$$S_k = \sinh(kh), \; S_a = \sinh(ah), \; C_k = \cosh(kh), \; C_a = \cosh(ah), \; K = \sigma + 2ik^2\nu_e, \; a^2 = k^2 - \frac{i\sigma}{\nu_e}, \text{ and } \nu_e = \nu + \frac{iG}{\rho\sigma}.$$

G is the shear modulus.

IC5 is based on Mosig et al. (2015), and the dispersion relation is defined as follows according to the WW3 manual:

$$Qgk\tanh(kd) - \sigma^2 = 0, \text{ where } Q = \frac{G_\nu h_i^3}{6\rho_w g}(1+\phi)k^4 - \frac{\rho h_i\sigma^2}{\rho_w g} + 1 \text{ and } G_\nu = G - i\sigma\rho\nu.$$

Appendix C: OSISAF-AMSR2 noise in open ocean

The OSISAF-AMSR2 SIC estimates during the November 2018 study period consist of prevalent erroneous estimates in the open ocean. At the R/V Mirai positions, inaccurate SIC is estimated on 14 and 20 November 2018 when R/V Mirai was not in ice cover. These estimates are noise because SSTs were too warm for new and young ice to form, so only perennial ice could survive. R/V Mirai has strenuous restrictions on sailing near first-year and perennial sea ice, and the sightings of them are logged by the experienced ice navigator. This is supported by the wave model as the TodaiWW3-ArCS simulation using OSISAF-AMSR2 as forcing calculates H_{m0} interpolated at R/V Mirai as 0 m for the 14 November on-ice event as shown in Figure A1. There is also apparent H_{m0} errors on 20 November. The open ocean OSISAF-AMSR2 SIC estimates for 14 and 20 November are shown in Figure A2.

Appendix D: R/V Mirai MIZ transect sea ice observation and satellite retrieved SIC at the observation locations

This appendix describes the environmental conditions during the MIZ transect sea ice observation conducted by R/V Mirai in the refreezing Chukchi Sea, which is described in Section 2.1. It also provides the comparison of eight satellite retrieved SIC at the observation locations including those at the Piper#13 drifting wave buoy.

R/V Mirai began the 12-day sea ice observation on 9 November 2018. Coinciding with this schedule, the transect waters began to refreeze and became consolidated ice cover at the start and (several days after) end of the observation period. The sea ice observation is grouped in four phases as distinct ocean surface features were captured from four meteorological conditions the ship encountered. Figure A3 presents the shipboard measured wind and SST data as well as bilinearly interpolated (in space) ERA5 10 m wind speeds. During the first few days between 9 and 13 November 2018 (Phase 1), gradual sea ice growth was observed both in extent and ice cake/floe sizes under generally calm surface conditions. On 14 November, the most significant on-ice wind event during the transect period occurred. The peak wind speed measured by R/V Mirai was 18 ms^{-1}, and > 10 ms^{-1} winds persisted for roughly 18 hours at the ship location. WM-2 and Piper-C#15 H_{m0} both peaked > 2.00 m in ice cover indicating energetic sea state of this event. The MIZ was mostly broken up ice fields on the following day, which was followed by the most apparent sea ice advance on 16 November as a seemingly dense ice field was encountered. We've grouped this period, Phase 2, as the on-ice event and aftermath. During 17 and 18 November, sea ice observation was mostly open water; our conjecture is the sea ice disappeared by horizontal advection, but there is insufficient evidence to simply discard rapid melting or other processes. This period of minimal ice sighting is referred as Phase 3. In the final Phase 4, SSTs along the transect waters began to warm despite the persistent and strengthening cold off-ice winds. Air temperatures along the MIZ transect on 18—20 November were < -10 °C, but the shipboard SSTs exceeded 0 °C for the entire MIZ transect waters the ship traversed on 20 November.

Figures A4 to A6 present the full time series of satellite retrieved SIC interpolated in time to hourly intervals and bilinearly interpolated in space at the R/V Mirai positions for the MIZ transect sea ice observation period between 9–20 November 2018. The figure schematics follow Figure 2. Lastly, satellite retrieved SIC data at the Piper#13 drifting wave buoy locations also interpolated in time and space are shown in Figure A7.

Author contributions. TN formulated the study idea, conducted the analysis, and prepared the manuscript. TW contributed significantly to the analysis and the manuscript. TK and JI continually contributed to the formulation of the manuscript from the start. JI designed the R/V Mirai MIZ transect sea ice observational plan.

Competing interests. Authors declare we have no competing interests.

Acknowledgements. We thank the editor and two anonymous reviewers for their valuable and insightful comments to improve the manuscript. This work was sponsored by the Japanese Ministry of Education, Culture, Sports, Science, and Technology through the ArCS project. A part of this study was also conducted under JSPS KAKENHI Grant Number JP 16H02429. JI acknowledges support from the KAKENHI grant numbers 18H03745 and 18KK0292. The authors greatly appreciate the comprehensive data available freely on the web. Satellite retrieved SIC were obtained from these sources: Cavalieri et al. (1996); Meier et al. (2018); Comiso (2017); Hori et al. (2012); Spreen et al. (2008). Furthermore, the OSI-401-b and OSI-408 were used and are the product of the EUMETSAT Ocean and Sea Ice Satellite Application Facility. Sentinel-1 SAR data were downloaded from NOAA (2019). ERA5 data were downloaded from Copernicus (2019), and ARCMFC wave model data were obtained from ARCMFC (2019). We are grateful to the R/V Mirai crew on board MR18-05C who made the MIZ transect sea ice observation possible. Note that our research cruise was supported by the PPP contribution with ECMWF weather and sea ice forecasts and Environment and Climate Change Canada sea ice forecast.

References

Andersen, S., Tonboe, R., Kaleschke, L., Heygster, G., and Pedersen, L. T.: Intercomparison of passive microwave sea ice concentration retrievals over the high-concentration Arctic sea ice, Journal of Geophysical Research: Oceans, 112, https://doi.org/10.1029/2006JC003543, 2007.

ARCMFC: Index of ftp://nrt.cmems-du.eu/Core/ARCTIC_ANALYSIS_FORECAST_WAV_002_010/dataset-wam-arctic-1hr6km-be/, [Online; accessed 11. Aug. 2019], 2019.

Ardhuin, F., Rogers, E., Babanin, A. V., Filipot, J.-F., Magne, R., Roland, A., van der Westhuysen, A., Queffeulou, P., Lefevre, J.-M., Aouf, L., and Collard, F.: Semiempirical Dissipation Source Functions for Ocean Waves. Part I: Definition, Calibration, and Validation, Journal of Physical Oceanography, 40, 1917–1941, https://doi.org/10.1175/2010JPO4324.1, 2010.

Ardhuin, F., Boutin, G., Stopa, J., Girard-Ardhuin, F., Melsheimer, C., Thomson, J., Kohout, A., Doble, M., and Wadhams, P.: Wave attenuation through an Arctic marginal ice zone on October 12, 2015: Part 2. Numerical modeling of waves and associated ice break-up, Journal of Geophysical Research: Oceans, https://doi.org/10.1002/2018JC013784, 2018.

Bekkers, E., Francois, J. F., and Rojas-Romagosa, H.: Melting Ice Caps and the Economic Impact of Opening the Northern Sea Route, The Economic Journal, 128, 1095–1127, https://doi.org/10.1111/ecoj.12460, 2018.

Boutin, G., Ardhuin, F., Dumont, D., Sevigny, C., Girard-Ardhuin, F., and Accensi, M.: Floe Size Effect on Wave-Ice Interactions: Possible Effects, Implementation in Wave Model, and Evaluation, Journal of Geophysical Research: Oceans, 123, 4779–4805, https://doi.org/10.1029/2017JC013622, 2018.

Boutin, G., Lique, C., Ardhuin, F., Rousset, C., Talandier, C., Accensi, M., and Girard-Ardhuin, F.: Toward a coupled model to investigate wave-sea ice interactions in the Arctic marginal ice zone, The Cryosphere Discussions, 2019, 1–39, https://doi.org/10.5194/tc-2019-92, 2019.

Canadian Ice Service-Environment Canada: Manual of Ice (MANICE). Manual of Standard Procedures for Observing and Reporting Ice Conditions, Tech. rep., Canadian Ice Service—Environment Canada, cATALOGUE NO. En56-175/2005, 2005.

Cavalieri, D. J., Gloersen, P., and Campbell, W. J.: Determination of sea ice parameters with the NIMBUS 7 SMMR, Journal of Geophysical Research: Atmospheres, 89, 5355–5369, https://doi.org/10.1029/JD089iD04p05355, 1984.

Cavalieri, D. J., Parkinson, C. L., Gloersen, P., and Zwally, H. J.: updated yearly. Sea Ice Concentrations from Nimbus-7 SMMR and DMSP SSM/I-SSMIS Passive Microwave Data, Version 1. November 2018. Arctic grid, https://doi.org/10.5067/8GQ8LZQVL0VL, [Date accessed 23. Jul. 2019], 1996.

Cheng, S., Rogers, W. E., Thomson, J., Smith, M., Doble, M. J., Wadhams, P., Kohout, A. L., Lund, B., Persson, O. P., Collins III, C. O., Ackley, S. F., Montiel, F., and Shen, H. H.: Calibrating a Viscoelastic Sea Ice Model for Wave Propagation in the Arctic Fall Marginal Ice Zone, Journal of Geophysical Research: Oceans, 122, 8770–8793, https://doi.org/doi/abs/10.1002/2017JC013275, 2017.

Chevallier, M., Smith, G. C., Dupont, F., Lemieux, J.-F., Forget, G., Fujii, Y., Hernandez, F., Msadek, R., Peterson, K. A., Storto, A., Toyoda, T., Valdivieso, M., Vernieres, G., Zuo, H., Balmaseda, M., Chang, Y.-S., Ferry, N., Garric, G., Haines, K., Keeley, S., Kovach, R. M., Kuragano, T., Masina, S., Tang, Y., Tsujino, H., and Wang, X.: Intercomparison of the Arctic sea ice cover in global ocean–sea ice reanalyses from the ORA-IP project, Climate Dynamics, 49, 1107–1136, https://doi.org/10.1007/s00382-016-2985-y, 2017.

Collins III, C. O., Rogers, W. E., Marchenko, A., and Babanin, A. V.: In situ measurements of an energetic wave event in the Arctic marginal ice zone, Geophysical Research Letters, 42, 1863–1870, https://doi.org/10.1002/2015gl063063, 2015.

Comiso, J. C.: Characteristics of Arctic winter sea ice from satellite multispectral microwave observations, Journal of Geophysical Research: Oceans, 91, 975–994, https://doi.org/10.1029/JC091iC01p00975, 1986.

Comiso, J. C.: Enhanced Sea Ice Concentrations from Passive Microwave Data, Tech. rep., NASA Goddard Space Flight Center, https://nsidc.org/sites/nsidc.org/files/files/data/pm/Bootstrap_Algorithm_Revised07.pdf, 2007.

Comiso, J. C.: Bootstrap Sea Ice Concentrations from Nimbus-7 SMMR and DMSP SSM/I-SSMIS, Version 3. November 2018. Arctic grid, https://doi.org/10.5067/7Q8HCCWS4I0R, [Date accessed 23. Jul. 2019], 2017.

Comiso, J. C., Cavalieri, D. J., Parkinson, C. L., and Gloersen, P.: Passive microwave algorithms for sea ice concentration: A comparison of two techniques, Remote Sensing of Environment, 60, 357 – 384, https://doi.org/10.1016/S0034-4257(96)00220-9, 1997.

Comiso, J. C., Meier, W. N., and Gersten, R.: Variability and trends in the Arctic Sea ice cover: Results from different techniques, Journal of Geophysical Research: Oceans, 122, 6883–6900, https://doi.org/10.1002/2017JC012768, 2017.

Copernicus: ERA5 hourly data on single levels from 1979 to present, https://cds.climate.copernicus.eu/cdsapp#!/dataset/reanalysis-era5-single-levels?tab=overview, [Online; accessed 11. Aug. 2019], 2019.

Donlon, C. J., Martin, M., Stark, J., Roberts-Jones, J., Fiedler, E., and Wimmer, W.: The Operational Sea Surface Temperature and Sea Ice Analysis (OSTIA) system, Remote Sensing of Environment, 116, 140 – 158, https://doi.org/10.1016/j.rse.2010.10.017, 2012.

Dumont, D., Kohout, A., and Bertino, L.: A wave-based model for the marginal ice zone including a floe breaking parameterization, Journal of Geophysical Research: Oceans, 116, https://doi.org/10.1029/2010JC006682, 2011.

Guest, P., Persson, P. O. G., Wang, S., Jordan, M., Jin, Y., Blomquist, B., and Fairall, C.: Low-Level Baroclinic Jets Over the New Arctic Ocean, Journal of Geophysical Research: Oceans, 123, 4074–4091, https://doi.org/10.1002/2018JC013778, 2018.

Heygster, G., Huntemann, M., Ivanova, N., Saldo, R., and Pedersen, L. T.: Response of passive microwave sea ice concentration algorithms to thin ice, in: 2014 IEEE Geoscience and Remote Sensing Symposium, pp. 3618–3621, https://doi.org/10.1109/IGARSS.2014.6947266, 2014.

Hori, M., Yabuki, H., Sugimura, T., and Terui, T.: AMSR2 Level 3 product of Daily Polar Brightness Temperatures and Product, 1.00, https://ads.nipr.ac.jp/dataset/A20170123-003, [Date accessed 23. Jul. 2019], 2012.

Inoue, J., Hori, M. E., Enomoto, T., and Kikuchi, T.: Intercomparison of Surface Heat Transfer Near the Arctic Marginal Ice Zone for Multiple Reanalyses: A Case Study of September 2009, SOLA, 7, 57–60, https://doi.org/10.2151/sola.2011-015, 2011.

Ivanova, N., Pedersen, L. T., Tonboe, R. T., Kern, S., Heygster, G., Lavergne, T., Sørensen, A., Saldo, R., Dybkjær, G., Brucker, L., and Shokr, M.: Inter-comparison and evaluation of sea ice algorithms: towards further identification of challenges and optimal approach using passive microwave observations, The Cryosphere, 9, 1797–1817, https://doi.org/10.5194/tc-9-1797-2015, 2015.

Jakobsson, M., Mayer, L., Coakley, B., Dowdeswell, J. A., Forbes, S., Fridman, B., Hodnesdal, H., Noormets, R., Pedersen, R., Rebesco, M., Schenke, H. W., Zarayskaya, Y., Accettella, D., Armstrong, A., Anderson, R. M., Bienhoff, P., Camerlenghi, A., Church, I., Edwards, M., Gardner, J. V., Hall, J. K., Hell, B., Hestvik, O., Kristoffersen, Y., Marcussen, C., Mohammad, R., Mosher, D., Nghiem, S. V., Pedrosa, M. T., Travaglini, P. G., and Weatherall, P.: The International Bathymetric Chart of the Arctic Ocean (IBCAO) Version 3.0, Geophysical Research Letters, 39, L12609, https://doi.org/10.1029/2012GL052219, 2012.

JAMSTEC: R/V Mirai Cruise Report MR18-05C Arctic Challenge and for Sustainability (ArCS). Arctic Ocean, Bering Sea, and North Pacific. 24 October–7 December2018, Tech. rep., Japan Agency for Marine-Earth Science and Technology (JAMSTEC), http://www.godac.jamstec.go.jp/catalog/data/doc_catalog/media/MR18-05C_all.pdf, 2018.

JAMSTEC: Oceanographic Research Vessel MIRAI, https://www.jamstec.go.jp/e/about/equipment/ships/mirai.html, [Online; accessed 22. Jul. 2019], 2019.

Jones, E., Oliphant, T., Peterson, P., et al.: SciPy: Open source scientific tools for Python, http://www.scipy.org/, [Online; accessed 23. July. 2019], 2001–.

Jung, T., Gordon, N. D., Bauer, P., Bromwich, D. H., Chevallier, M., Day, J. J., Dawson, J., Doblas-Reyes, F., Fairall, C., Goessling, H. F., Holland, M., Inoue, J., Iversen, T., Klebe, S., Lemke, P., Losch, M., Makshtas, A., Mills, B., Nurmi, P., Perovich, D., Reid, P., Renfrew, I. A., Smith, G., Svensson, G., Tolstykh, M., and Yang, Q.: Advancing Polar Prediction Capabilities on Daily to Seasonal Time Scales, Bulletin of the American Meteorological Society, 97, 1631–1647, https://doi.org/10.1175/BAMS-D-14-00246.1, 2016.

Kohout, A. L., Penrose, B., Penrose, S., and Williams, M. J.: A device for measuring wave-induced motion of ice floes in the Antarctic Marginal Ice Zone, Annals of Glaciology, 56, 415–424, https://doi.org/10.3189/2015aog69a600, 2015.

Kwok, R. and Rothrock, D. A.: Decline in Arctic sea ice thickness from submarine and ICESat records: 1958–2008, Geophysical Research Letters, 36, https://doi.org/10.1029/2009GL039035, 2009.

Lavergne, T., Sørensen, A. M., Kern, S., Tonboe, R., Notz, D., Aaboe, S., Bell, L., Dybkjær, G., Eastwood, S., Gabarro, C., Heygster, G., Killie, M. A., Brandt Kreiner, M., Lavelle, J., Saldo, R., Sandven, S., and Pedersen, L. T.: Version 2 of the EUMETSAT OSI SAF and ESA CCI sea-ice concentration climate data records, The Cryosphere, 13, 49–78, https://doi.org/10.5194/tc-13-49-2019, 2019.

Li, J., Kohout, A. L., Doble, M. J., Wadhams, P., Guan, C., and Shen, H. H.: Rollover of Apparent Wave Attenuation in Ice Covered Seas, Journal of Geophysical Research: Oceans, 122, 8557–8566, https://doi.org/10.1002/2017JC012978, 2017.

Liu, A. K. and Mollo-Christensen, E.: Wave Propagation in a Solid Ice Pack, Journal of Physical Oceanography, 18, 1702–1712, https://doi.org/10.1175/1520-0485(1988)018<1702:WPIASI>2.0.CO;2, 1988.

Liu, Q., Rogers, W. E., Babanin, A. V., Young, I. R., Romero, L., Zieger, S., Qiao, F., and Guan, C.: Observation-Based Source Terms in the Third-Generation Wave Model WAVEWATCH III: Updates and Verification, Journal of Physical Oceanography, 49, 489–517, https://doi.org/10.1175/JPO-D-18-0137.1, 2019.

Maslanik, J. A., Fowler, C., Stroeve, J., Drobot, S., Zwally, J., Yi, D., and Emery, W.: A younger, thinner Arctic ice cover: Increased potential for rapid extensive sea-ice loss, Geophysical Research Letters, 34, https://doi.org/10.1029/2007GL032043, 2007.

Meier, W. N.: Comparison of passive microwave ice concentration algorithm retrievals with AVHRR imagery in Arctic peripheral seas, IEEE Transactions on Geoscience and Remote Sensing, 43, 1324–1337, https://doi.org/10.1109/TGRS.2005.846151, 2005.

Meier, W. N., Markus, T., and Comiso, J. C.: AMSR-E/AMSR2 Unified L3 Daily 12.5 km Brightness Temperatures, Sea Ice Concentration, Motion & Snow Depth Polar Grids, Version 1. November 2018. Arctic grid, https://doi.org/10.5067/RA1MIJOYPK3P, [Date accessed 23. Jul. 2019], 2018.

Meylan, M. H. and Masson, D.: A linear Boltzmann equation to model wave scattering in the marginal ice zone, Ocean Modelling, 11, 417 – 427, https://doi.org/10.1016/j.ocemod.2004.12.008, 2006.

Montiel, F., Squire, V. A., Doble, M., Thomson, J., and Wadhams, P.: Attenuation and Directional Spreading of Ocean Waves During a Storm Event in the Autumn Beaufort Sea Marginal Ice Zone, Journal of Geophysical Research: Oceans, 123, 5912–5932, https://agupubs.onlinelibrary.wiley.com/doi/abs/10.1029/2018JC013763, https://doi.org/10.1029/2018JC013763, 2018.

Mosig, J. E. M., Montiel, F., and Squire, V. A.: Comparison of viscoelastic-type models for ocean wave attenuation in ice-covered seas, Journal of Geophysical Research: Oceans, 120, 6072–6090, https://doi.org/10.1002/2015JC010881, 2015.

NOAA: Index of ftp://ftpcoastwatch.noaa.gov/pub/socd6/coastwatch/s1/sar/nrcs/2018/, [Online; accessed 10. Aug. 2019], 2019.

Nose, T., Webb, A., Waseda, T., Inoue, J., and Sato, K.: Predictability of storm wave heights in the ice-free Beaufort Sea, Ocean Dynamics, 68, 1383–1402, https://doi.org/10.1007/s10236-018-1194-0, 2018.

Notz, D.: Sea-ice extent and its trend provide limited metrics of model performance, The Cryosphere, 8, 229–243, https://doi.org/10.5194/tc-8-229-2014, 2014.

Rascle, N. and Ardhuin, F.: A global wave parameter database for geophysical applications. Part 2: Model validation with improved source term parameterization, Ocean Modelling, 70, 174 – 188, https://doi.org/10.1016/j.ocemod.2012.12.001, 2013.

Roach, L. A., Dean, S. M., and Renwick, J. A.: Consistent biases in Antarctic sea ice concentration simulated by climate models, The Cryosphere, 12, 365–383, 2018.

Roach, L. A., Bitz, C. M., Horvat, C., and Dean, S. M.: Advances in Modeling Interactions Between Sea Ice and Ocean Surface Waves, Journal of Advances in Modeling Earth Systems, 11, 4167–4181, https://doi.org/10.1029/2019MS001836, 2019.

Rogers, W. E. and Campbell, T. J.: Implementation of curvilinear coordinate system in the WAVEWATCH III model, Tech. Rep. NRL/MR/7320–09-9193, Naval Research Laboratory, Stennis Space Center, 2009.

Rogers, W. E., Babanin, A. V., and Wang, D. W.: Observation-Consistent Input and Whitecapping Dissipation in a Model for Wind-Generated Surface Waves: Description and Simple Calculations, Journal of Atmospheric and Oceanic Technology, 29, 1329–1346, https://doi.org/10.1175/JTECH-D-11-00092.1, 2012.

Rogers, W. E., Thomson, J., Shen, H. H., Doble, M. J., Wadhams, P., and Cheng, S.: Dissipation of wind waves by pancake and frazil ice in the autumn Beaufort Sea, Journal of Geophysical Research: Oceans, 121, 7991–8007, https://doi.org/10.1002/2016jc012251, 2016.

Spreen, G., Kaleschke, L., and Heygster, G.: Sea ice remote sensing using AMSR-E 89-GHz channels, Journal of Geophysical Research: Oceans, 113, https://doi.org/10.1029/2005JC003384, 2008.

Squire, V. A.: A fresh look at how ocean waves and sea ice interact, Philosophical Transactions of the Royal Society A: Mathematical, Physical and Engineering Sciences, 376, 20170 342, https://doi.org/10.1098/rsta.2017.0342, 2018.

Stephenson, S. R., Smith, L. C., Brigham, L. W., and Agnew, J. A.: Projected 21st-century changes to Arctic marine access, Climatic Change, 118, 885–899, https://doi.org/10.1007/s10584-012-0685-0, 2013.

Stroeve, J. and Notz, D.: Changing state of Arctic sea ice across all seasons, Environmental Research Letters, 13, 103 001, https://doi.org/10.1088/1748-9326/aade56, 2018.

Stroeve, J. C., Serreze, M. C., Holland, M. M., Kay, J. E., Malanik, J., and Barrett, A. P.: The Arctic's rapidly shrinking sea ice cover: a research synthesis, Climatic Change, 110, 1005–1027, https://doi.org/10.1007/s10584-011-0101-1, 2012.

Sutherland, G., Rabault, J., Christensen, K. H., and Jensen, A.: A two layer model for wave dissipation in sea ice, Applied Ocean Research, 88, 111 – 118, https://doi.org/10.1016/j.apor.2019.03.023, 2019.

The WAVEWATCH III® Development Group (WW3DG): User manual and system documentation of WAVEWATCH III ® version 6.07, Tech. Note 333, NOAA/NWS/NCEP/MMAB, College Park, MD, USA, 465 pp. + Appendices, 2019.

Thomson, J., Ackley, S., Girard-Ardhuin, F., Ardhuin, F., Babanin, A., Boutin, G., Brozena, J., Cheng, S., Collins, C., Doble, M., Fairall, C., Guest, P., Gebhardt, C., Gemmrich, J., Graber, H. C., Holt, B., Lehner, S., Lund, B., Meylan, M. H., Maksym, T., Montiel, F., Perrie, W., Persson, O., Rainville, L., Erick Rogers, W., Shen, H., Shen, H., Squire, V., Stammerjohn, S., Stopa, J., Smith, M. M., Sutherland, P., and Wadhams, P.: Overview of the Arctic Sea State and Boundary Layer Physics Program, Journal of Geophysical Research: Oceans, 123, 8674–8687, https://doi.org/10.1002/2018JC013766, 2018.

TSK Tsurumi Seiki Co., Ltd.: Oceanographic Equipment Water Quality Monitoring Equipment | TSK Tsurumi Seiki Co., Ltd. - Microwave Type Wave Height Meter WM-2, http://www.tsk-jp.com/index.php?page=/product/detail/21/2, [Online; accessed 23. Jul. 2019], 2019.

V.A. Squire: Of ocean waves and sea-ice revisited, Cold Regions Science and Technology, 49, 110 – 133, https://doi.org/10.1016/j.coldregions.2007.04.007, 2007.

Wang, R. and Shen, H. H.: Gravity waves propagating into an ice-covered ocean: A viscoelastic model, Journal of Geophysical Research: Oceans, 115, 10.1029/2009JC005591, 2010.

Wessel, P. and Smith, W. H. F.: A global, self-consistent, hierarchical, high-resolution shoreline database, Journal of Geophysical Research: Solid Earth, 101, 8741–8743, https://doi.org/10.1029/96JB00104, 1996.

Williams, T. D., Bennetts, L. G., Squire, V. A., Dumont, D., and Bertino, L.: Wave–ice interactions in the marginal ice zone. Part 1: Theoretical foundations, Ocean Modelling, 71, 81 – 91, https://doi.org/10.1016/j.ocemod.2013.05.010, 2013.

WMO: WMO Sea-Ice Nomenclature, Tech. Rep. 259, The Joint Technical Commission for Oceanography and Marine Meteorology (JCOMM), https://www.jcomm.info/index.php?option=com_oe&task=viewDocumentRecord&docID=14598, [Online; accessed 22. Jan. 2020], 2014.

Zhang, Y., Chen, C., Beardsley, R. C., Perrie, W., Gao, G., Zhang, Y., Qi, J., and Lin, H.: Applications of an unstructured grid surface wave model (FVCOM-SWAVE) to the Arctic Ocean: The interaction between ocean waves and sea ice, Ocean Modelling, 145, 101 532, https://doi.org/10.1016/j.ocemod.2019.101532, 2020.

Zieger, S., Babanin, A. V., Rogers, W. E., and Young, I. R.: Observation-based source terms in the third-generation wave model WAVEWATCH, Ocean Modelling, 96, 2 – 25, https://doi.org/10.1016/j.ocemod.2015.07.014, 2015.

FIGURES.

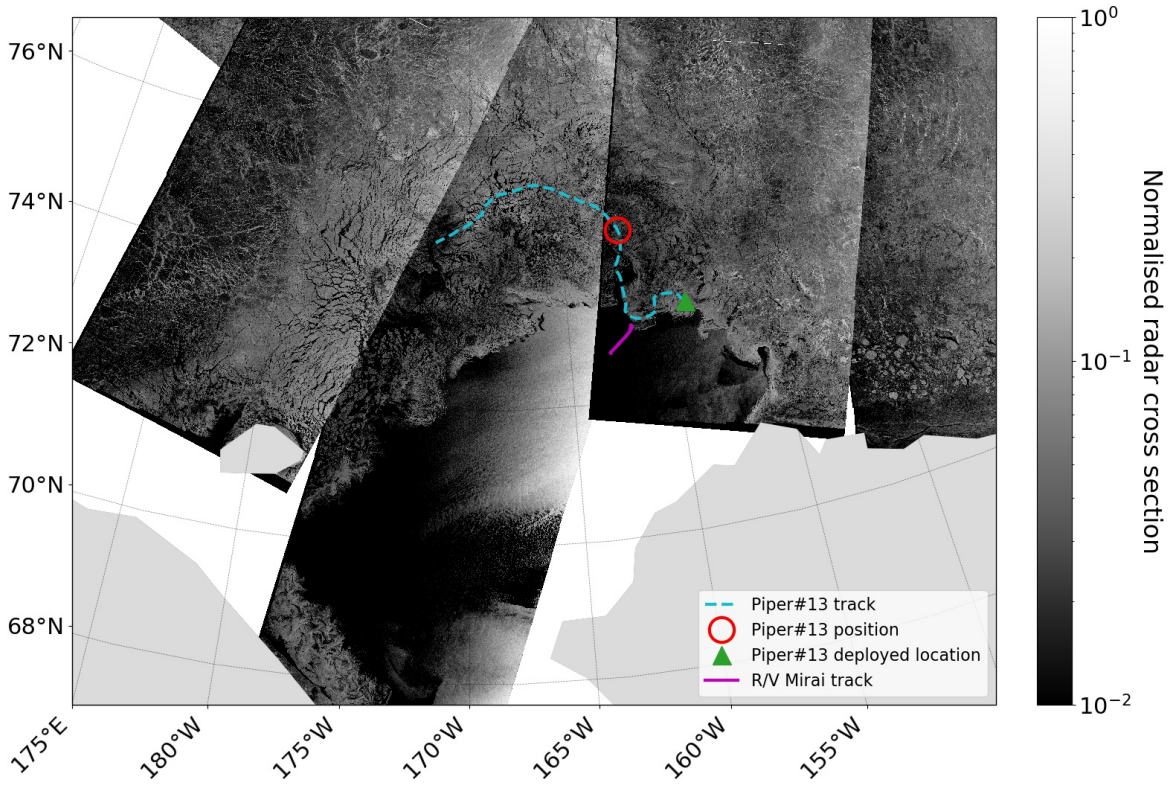

Figure 1. Observation locations are overlaid on the mosaic of Sentinel-1 NRCS images (NOAA, 2019) acquired on 15 November 2018. R/V Mirai track on this date is shown as the solid magenta line, and the Piper#13 drifting wave buoy track between 6–28 November is shown in the dashed cyan line. The green triangle shows the deployment location, and the red circle represents the buoy position on 15 November 12:00.

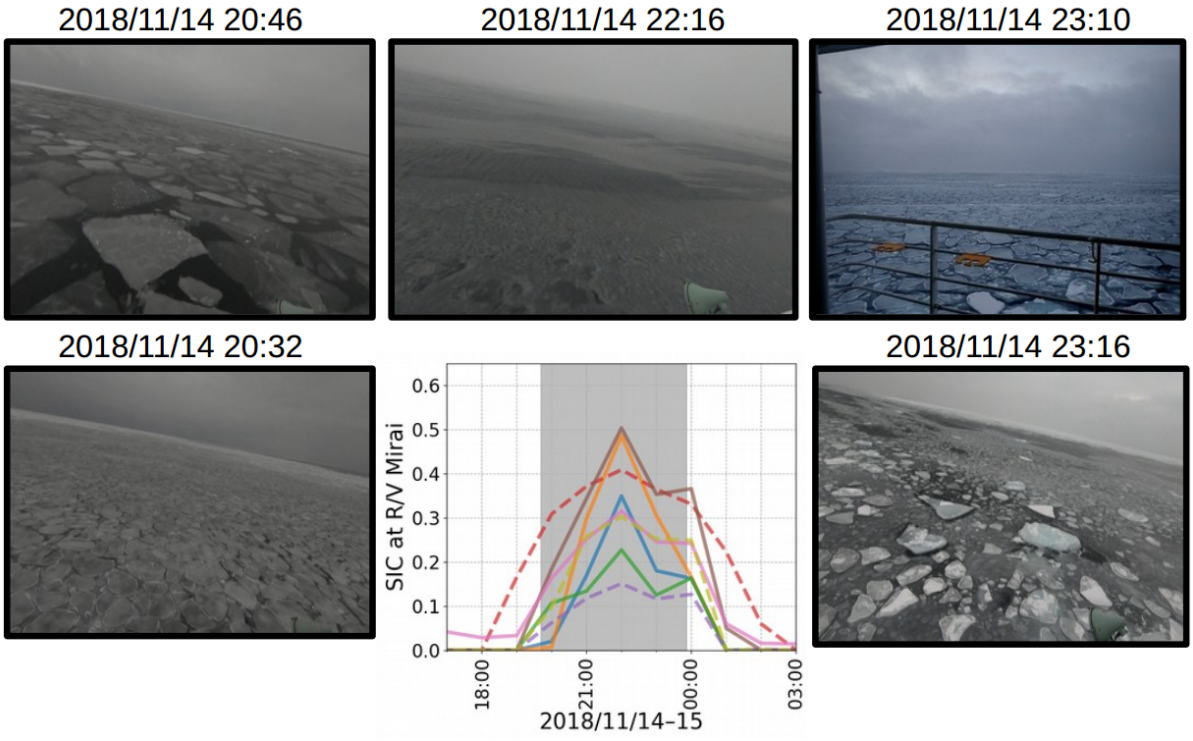

Figure 2. Snapshot images taken from R/V Mirai of the sea ice field and the satellite retrieved SIC estimates from eight products on 14 November 2018 during the on-ice wave event. The satellite derived SIC were linearly interpolated in time to hourly intervals and bilinearly interpolated in space from respective native grids to the R/V Mirai positions using the Python Scipy interpolation package (Jones et al., 2001–). The figure schematics of SIC estimates are as follows: ASI-3km (blue), ASI-6km (orange), BST-AMSR2 (green), BST-SSMIS (red), NT2-AMSR2 (purple), NT-SSMIS (brown), OSISAF-AMSR2 (pink), and OSISAF-SSMIS (olive), and SSMIS and AMSR2 are distinguished by dashed and solid lines, respectively. Grey highlighted times indicate when the vessel was in ice cover based on the ice navigator's logs: from the first (known) encounter of sea ice to the ship proceeding to the ice-free water.

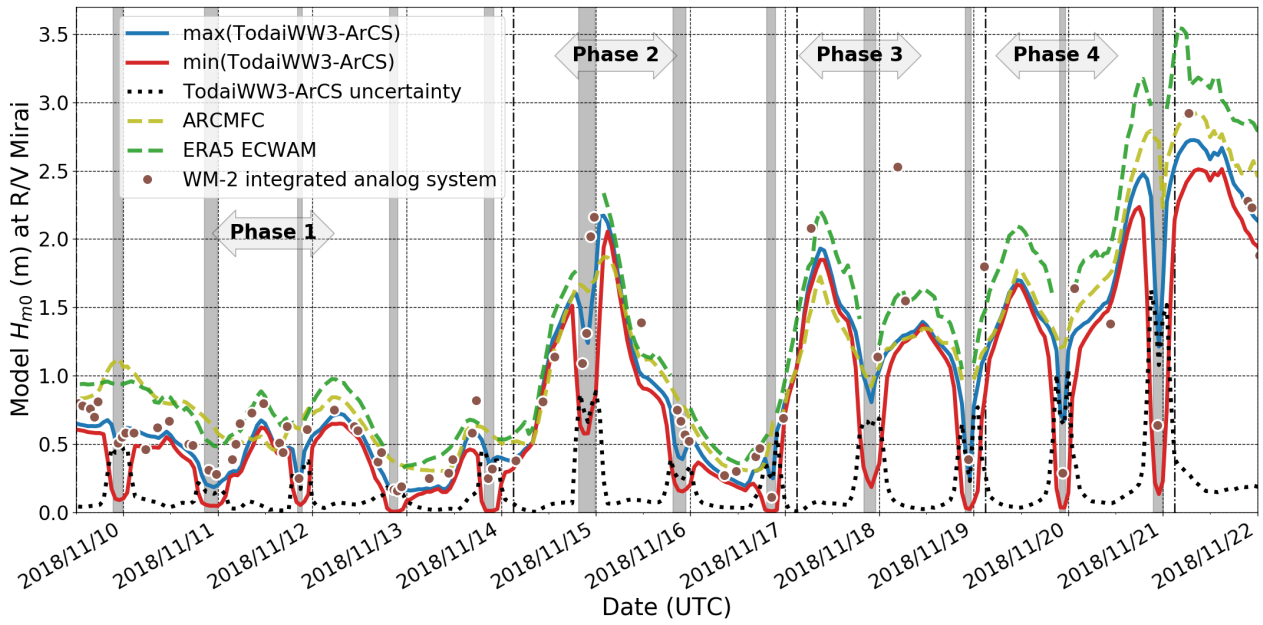

Figure 3. ΔH_{m0} of TodaiWW3-ArCS estimates using various SIC products as sea ice forcing interpolated at R/V Mirai positions are shown during the MIZ transect observation. The figure also shows the WM-2 data when R/V Mirai ship speed was < 2 ms^{-1} (refer to Appendix A for more details). Two independent predictions from ERA5 ECWAM and the ARCMFC wave model are also presented. Grey highlighted times indicate when the vessel was in ice-covered sea based on the ice navigator's logs. Refer to Appendix D for details on Phases.

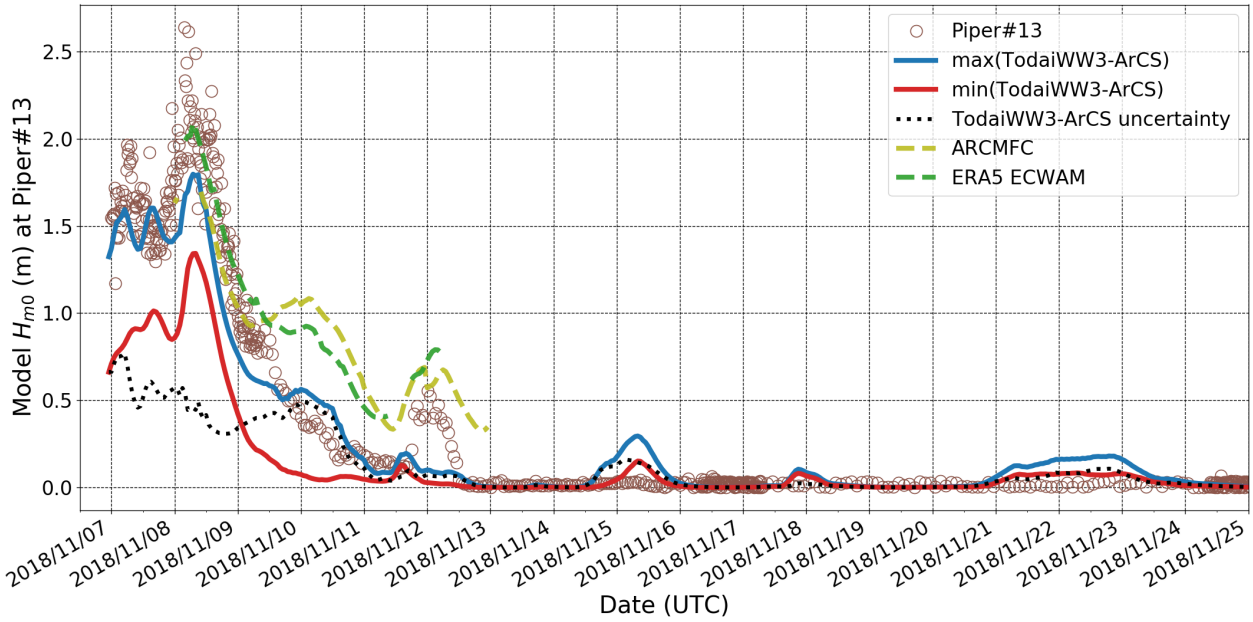

Figure 4. Piper#13 wave data are presented with TodaiWW3-ArCS ΔH_{m0} using various SIC products as sea ice forcing interpolated at the Piper#13 positions. Two independent predictions from ERA5 ECWAM and the ARCMFC wave model are also presented.

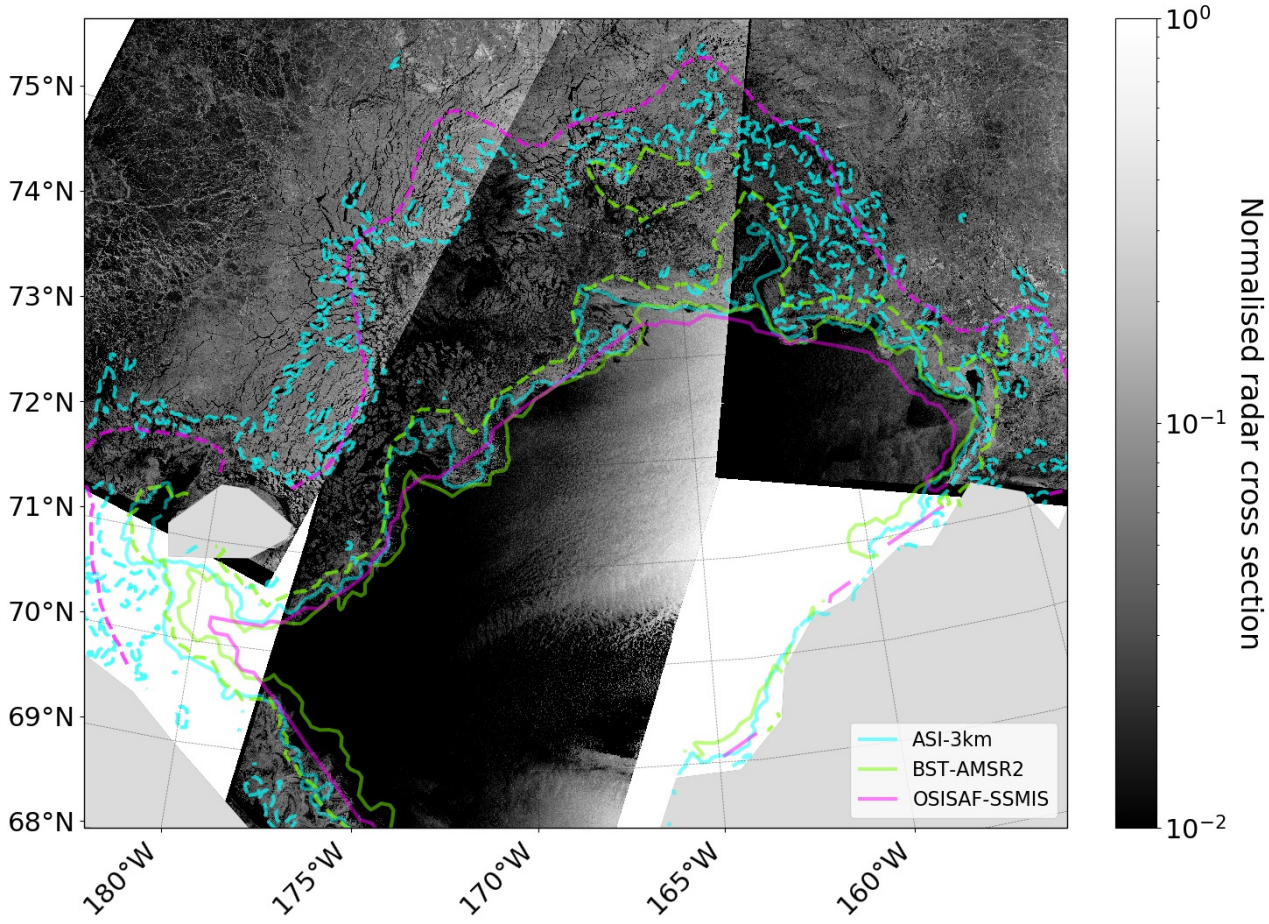

Figure 5. 0.15 (solid) and 0.85 (dashed) SIC contours of OSISAF-SSMIS, BST-AMSR2, and ASI-3km for 15 November 2018, shown respectively as magenta, lime green, and cyan lines, are overlaid on the mosaic of Sentinel-1 NRCS images (NOAA, 2019) acquired on the same day.

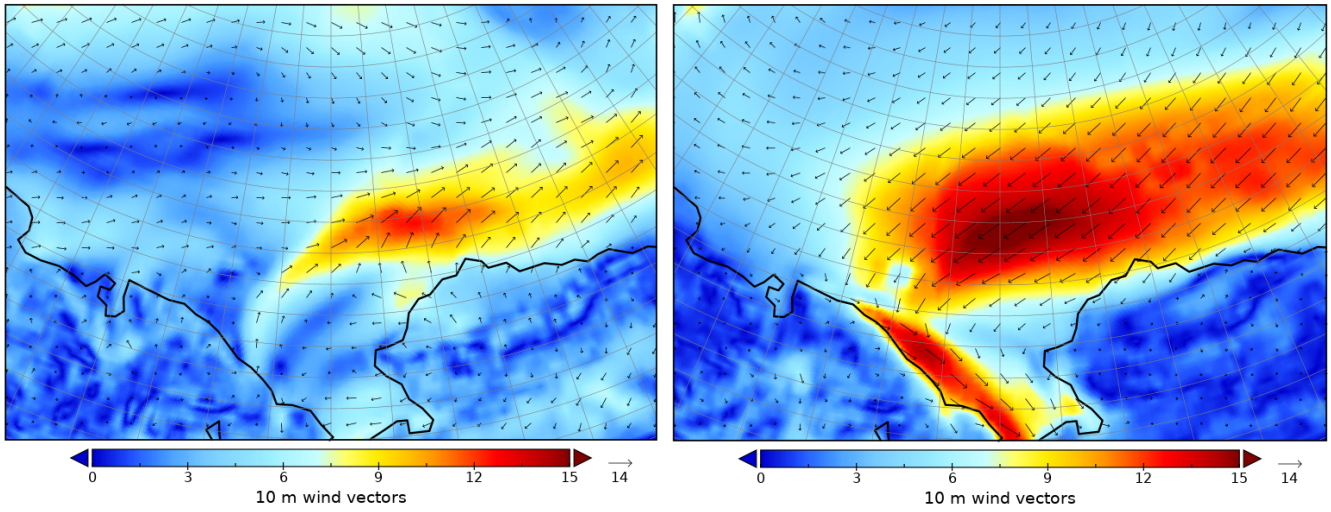

(a) South westerly on-ice winds on 15 November 2018 00:00.

(b) North easterly off-ice winds on 21 November 2018 21:00.

Figure 6. ERA5 10 m wind speed (ms^{-1}) and vectors to depict the forcing for the selected on- and off-ice wave cases.

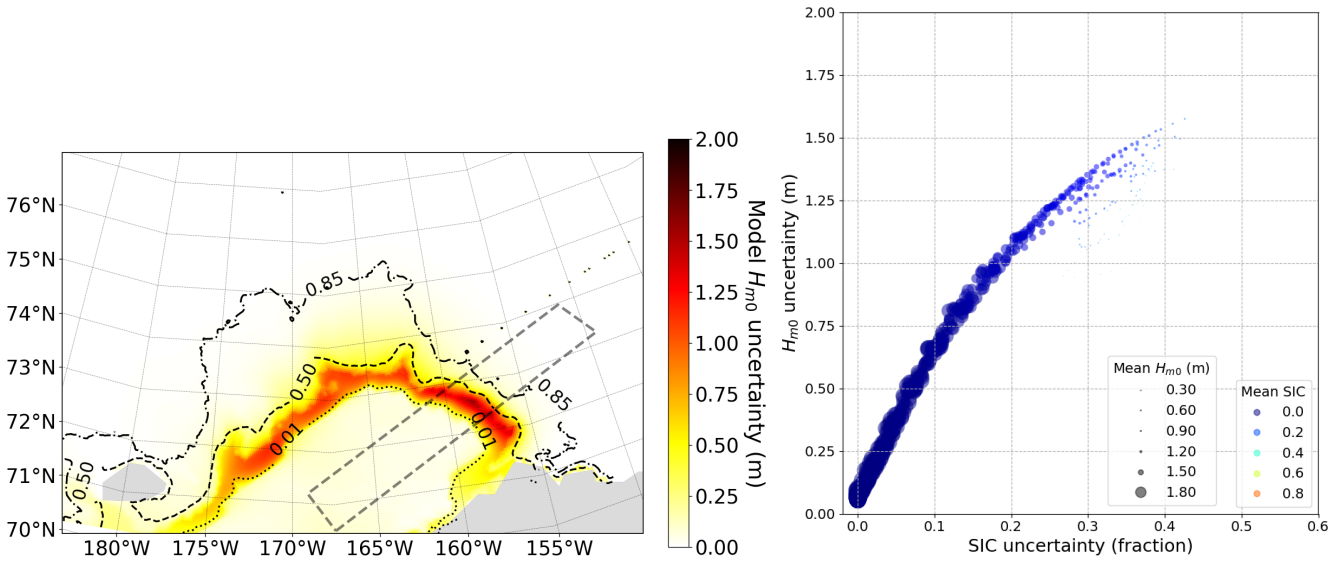

(a) TodaiWW3-ArCS ΔH_{m0} map with 0.01 (dotted), 0.50 (dashed), and 0.85 (dash-dotted) $mean(c_i)$ contours shown in black. Data enclosed in the grey dotted quadrilateral, which is orientated along the wind forcing direction, are plotted in Figure 7b.

(b) Bivariate model ΔH_{m0} and Δc_i uncertainty data for the on-ice wave case are shown in an enhanced scatter plot for the quadrilateral area in Figure 7a. The marker sizes are scaled by $mean(H_{m0})$, and the marker colours indicate $mean(c_i)$.

Figure 7. TodaiWW3-ArCS simulation on 15 November 2018 00:00 during on-ice south westerly wind conditions as shown in Figure 6a.

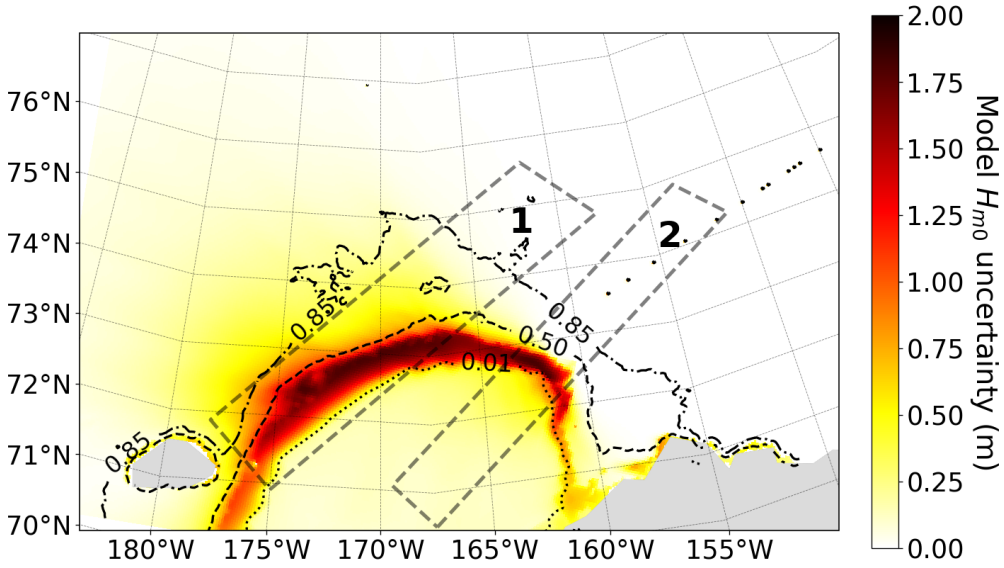

(a) TodaiWW3-ArCS ΔH_{m0} map with 0.01 (dotted), 0.50 (dashed), and 0.85 (dash-dotted) $mean(c_i)$ contours shown in black. Data enclosed in two grey dotted quadrilaterals are plotted in Figures 8b and 8c. Quadrilateral 1 depicts the region where the wind forcing is orientated along the ice edge, and Quadrilateral 2 reflects the off-ice wave case.

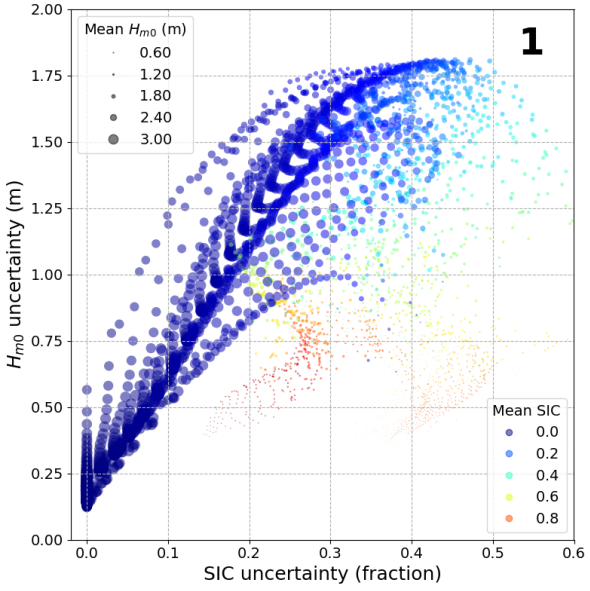

(b) Bivariate model ΔH_{m0} and Δc_i uncertainty data shown in an enhanced scatter plot for the Quadrilateral 1 area in Figure 8a where the wind forcing is orientated along the ice edge. The figure schematics follows Figure 7b.

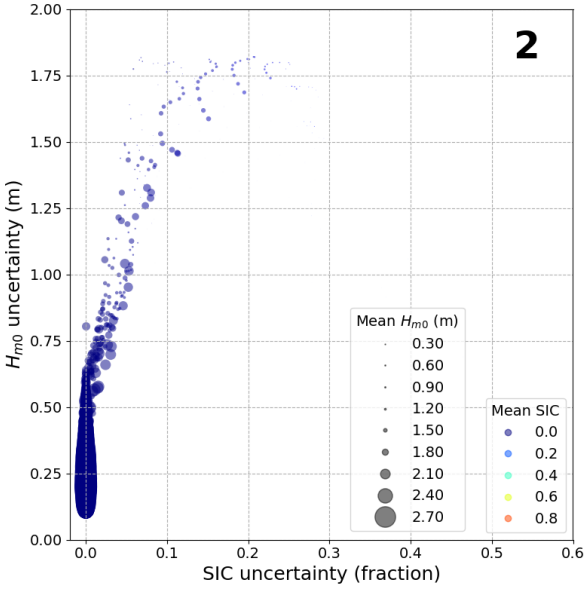

(c) Bivariate model ΔH_{m0} and Δc_i uncertainty data for the off-ice wave case are shown in an enhanced scatter plot for the Quadrilateral 2 area in Figure 8a. The figure schematics follows Figure 7b.

Figure 8. TodaiWW3-ArCS simulation on 21 November 2018 21:00 during north easterly off-ice wind conditions as shown in Figure 6b.

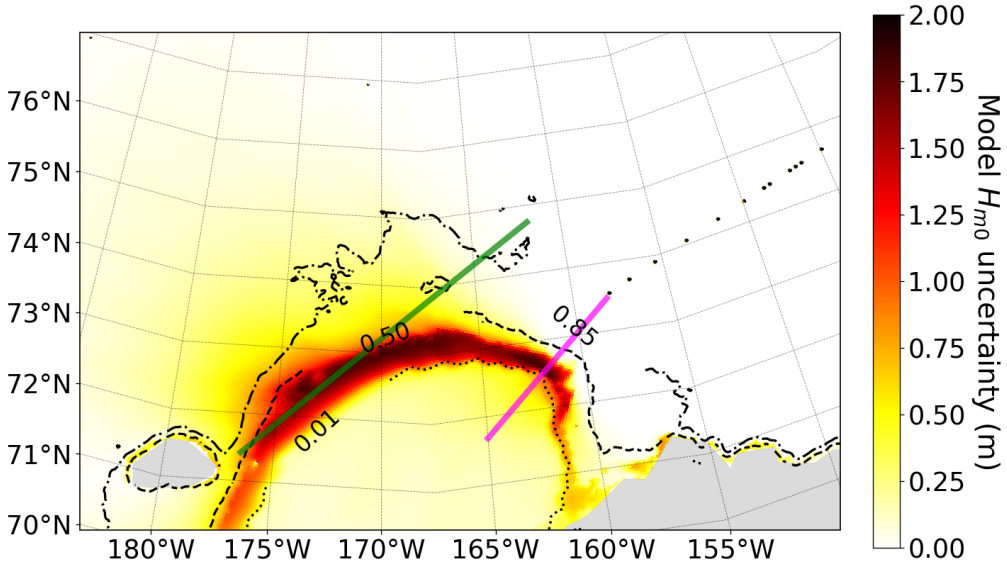

(a) TodaiWW3-ArCS H_{m0} uncertainty map with 0.01 (dotted), 0.50 (dashed), and 0.85 (dash-dotted) $mean(c_i)$ contours shown in black. Cross sections of H_{m0} and SIC c_i along the green and magenta transects are shown in Figures 9b and 9c, respectively.

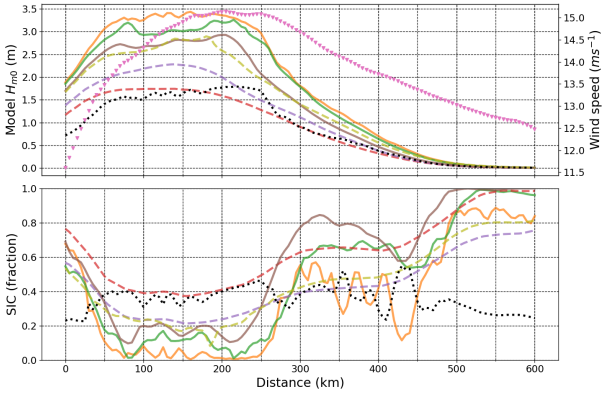

(b) Model H_{m0} (top) and SIC c_i (bottom) forcing along the green line in Figure 9a are shown for the Δc_i hindcast experiment. The figure schematics of SIC c_i forcing follow Figure 2. Magenta markers indicate the wind forcing magnitude, and dotted black lines represent ΔH_{m0} and Δc_i.

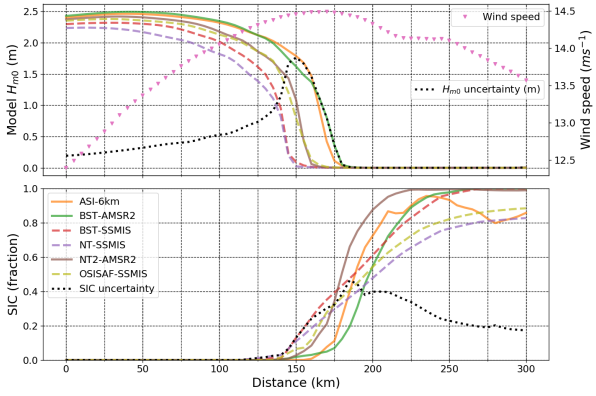

(c) Model H_{m0} (top) and SIC c_i (bottom) for an off-ice wave transect along the magenta line in Figure 9a are shown for the Δc_i hindcast experiment. The figure schematics follow Figure 9b.

Figure 9. TodaiWW3-ArCS simulation showing H_{m0} and SIC c_i transects on 21 November 2018 21:00 for the north easterly off-ice wave case.

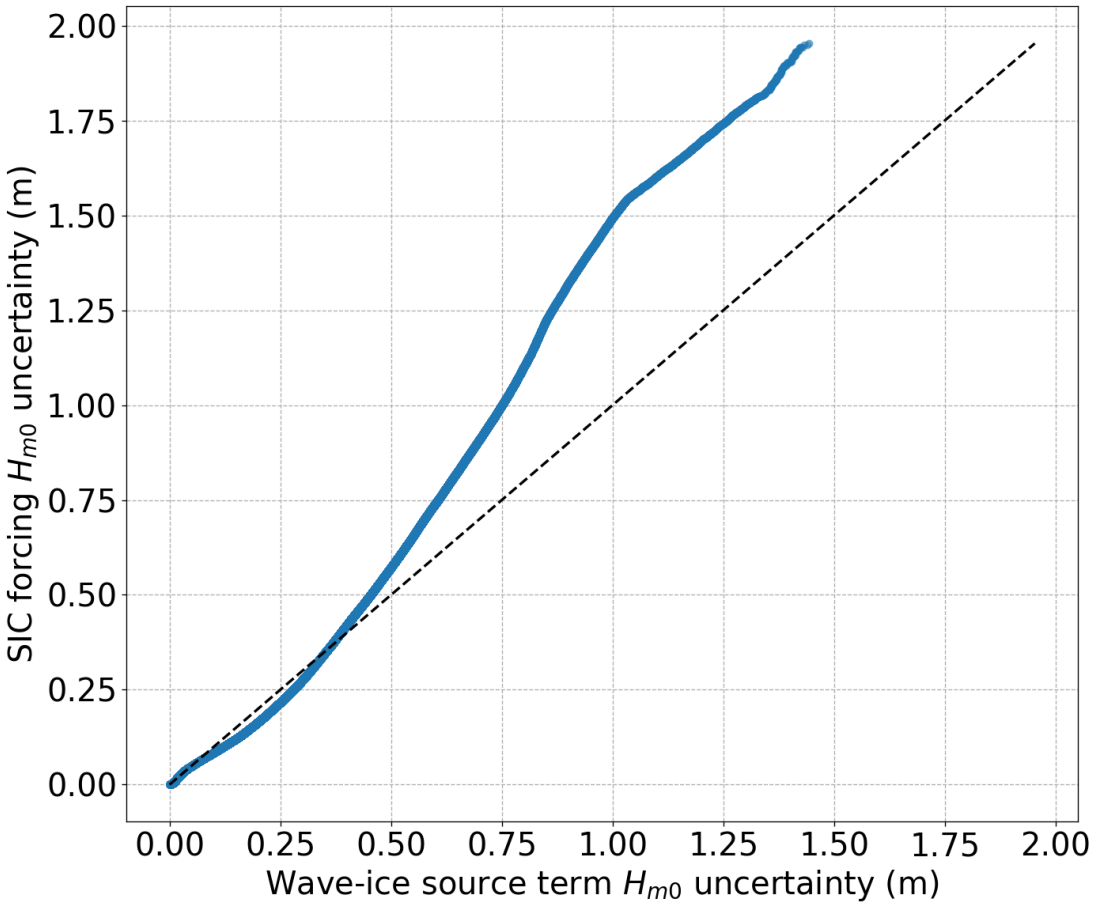

Figure 10. A Q-Q plot depicting the ΔH_{m0} distributions for Δc_i and s_{ice} uncertainty hindcast experiments.

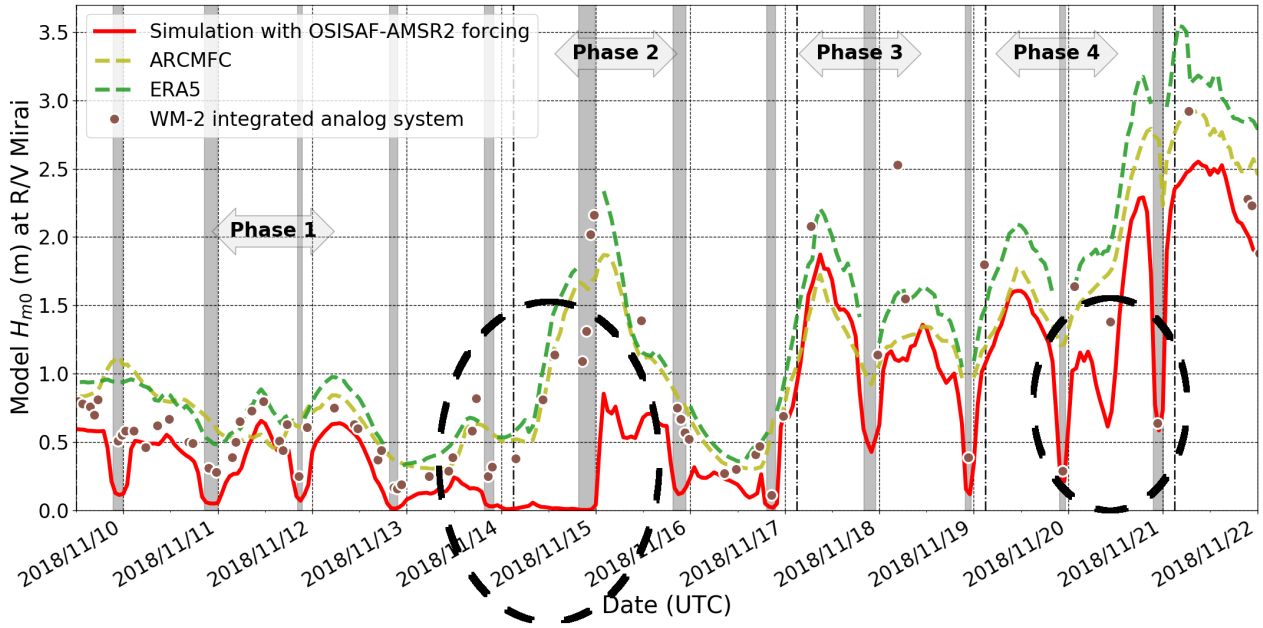

Figure A1. The TodaiWW3-ArCS H_{m0} estimates using the OSISAF-AMSR2 SIC as forcing interpolated at R/V Mirai positions are shown during the MIZ transect observation. The figure also shows the WM-2 data when R/V Mirai ship speed was < 2 ms^{-1}. Two independent predictions from ERA5 ECWAM and the ARCMFC wave model are also shown. Blacked dotted circles indicate times when the erroneous SIC forcing caused inaccurate estimates of H_{m0} at the R/V Mirai position. Grey highlighted times indicate when the vessel was in ice covered based on the ice navigator's logs: from the first (known) encounter of sea ice to the ship proceeding to the ice-free water.

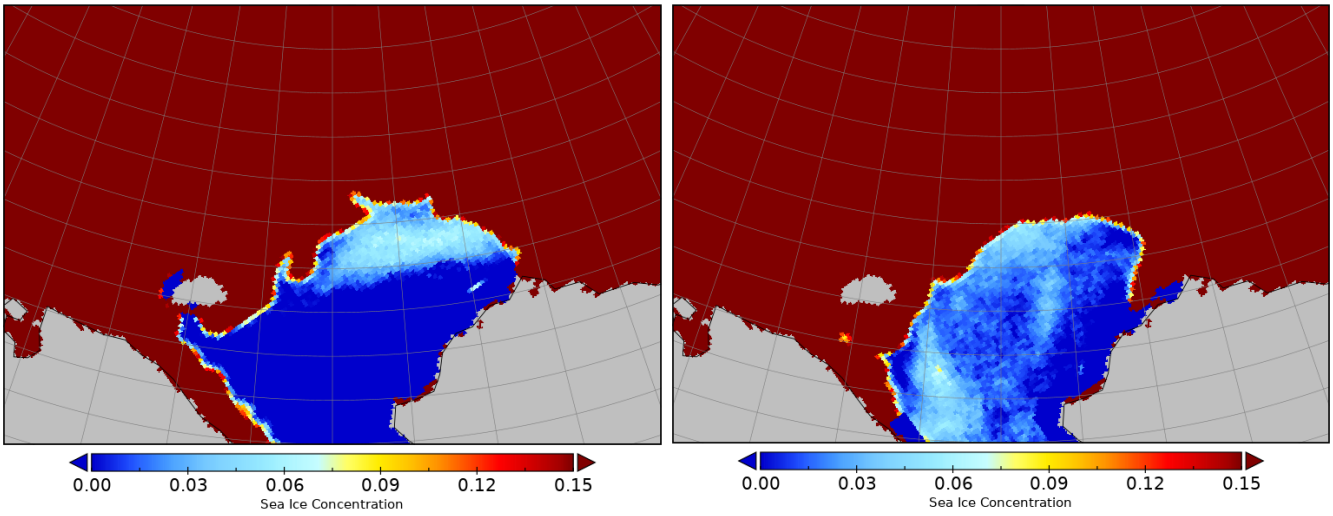

(a) SIC estimates on 15 November 2018.

(b) SIC estimates on 20 November 2018.

Figure A2. Apparent OSISAF-AMSR2 SIC noise in the open water during the R/V Mirai MIZ transect observation.

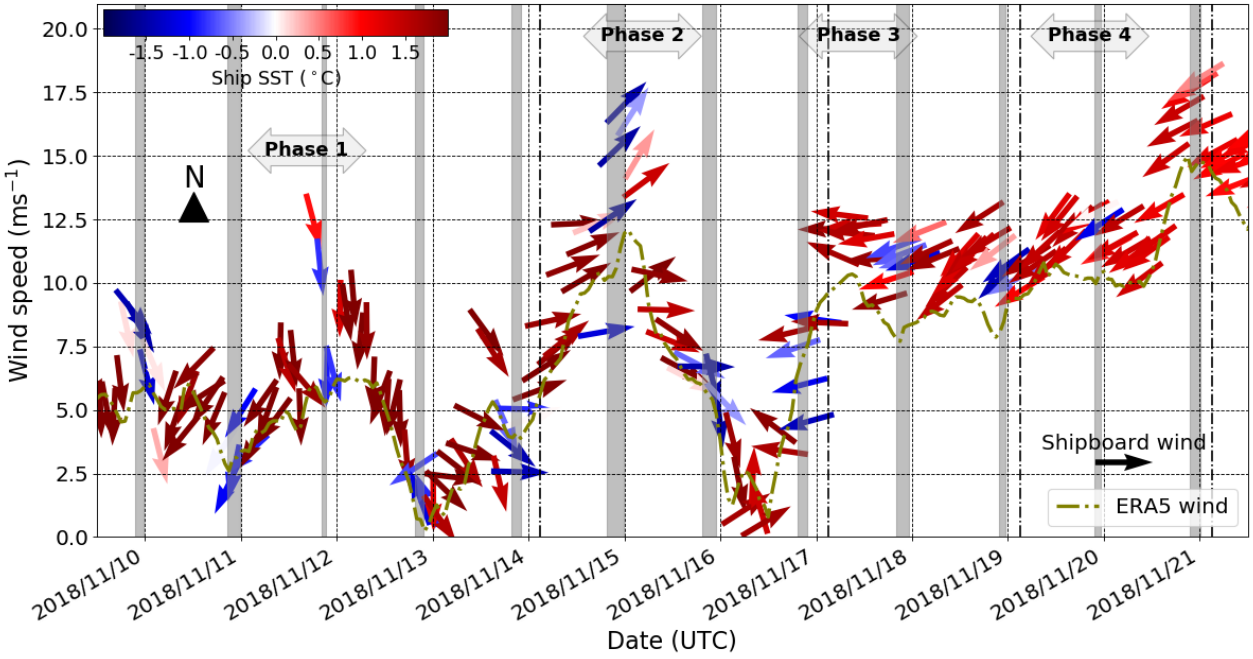

Figure A3. Shipboard wind and SST and bilinearly interpolated ERA5 10 m winds at the R/V Mirai position. Grey highlighted times indicate when the vessel was in ice cover based on the ice navigator's logs.

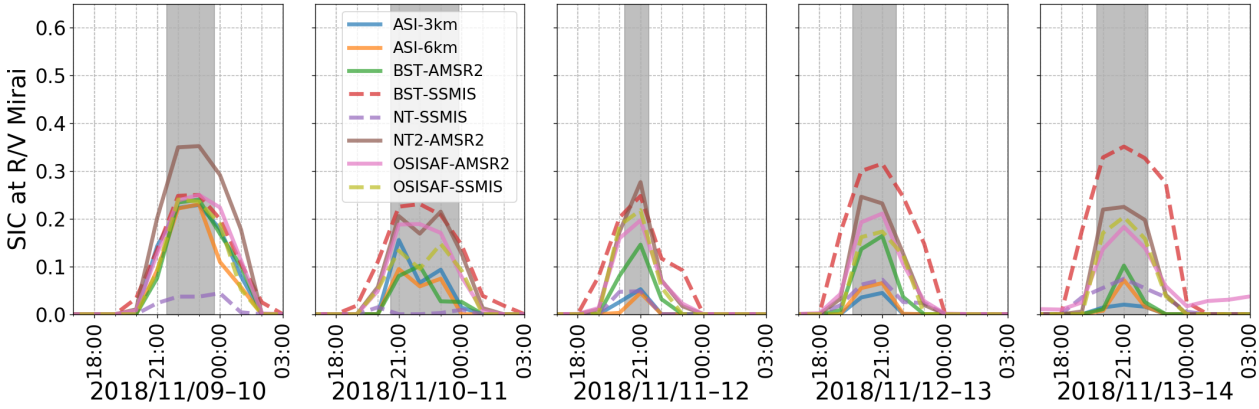

Figure A4. Satellite retrieved SIC for all products along the R/V Mirai track during Phase 1 between 9–13 November 2018. The figure schematics of SIC estimates are as follows: ASI-3km (blue), ASI-6km (orange), BST-AMSR2 (green), BST-SSMIS (red), NT2-AMSR2 (purple), NT-SSMIS (brown), OSISAF-AMSR2 (pink), and OSISAF-SSMIS (olive), and SSMIS and AMSR2 are distinguished by dashed and solid lines, respectively. Grey highlighted times indicate when the vessel was in ice cover based on the ice navigator's logs.

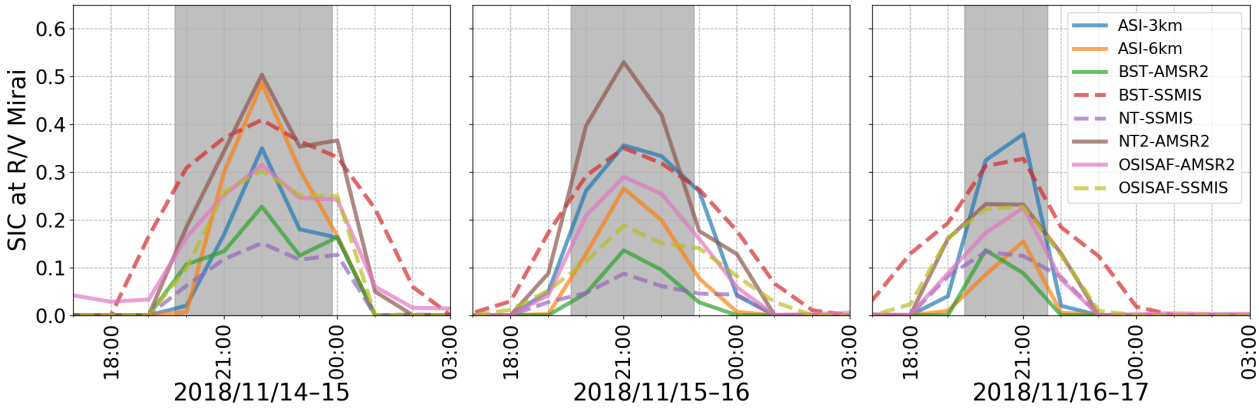

Figure A5. Satellite retrieved SIC for all products along the R/V Mirai track during Phase 2 between 14–16 November 2018. The figure schematics follow Figure A4.

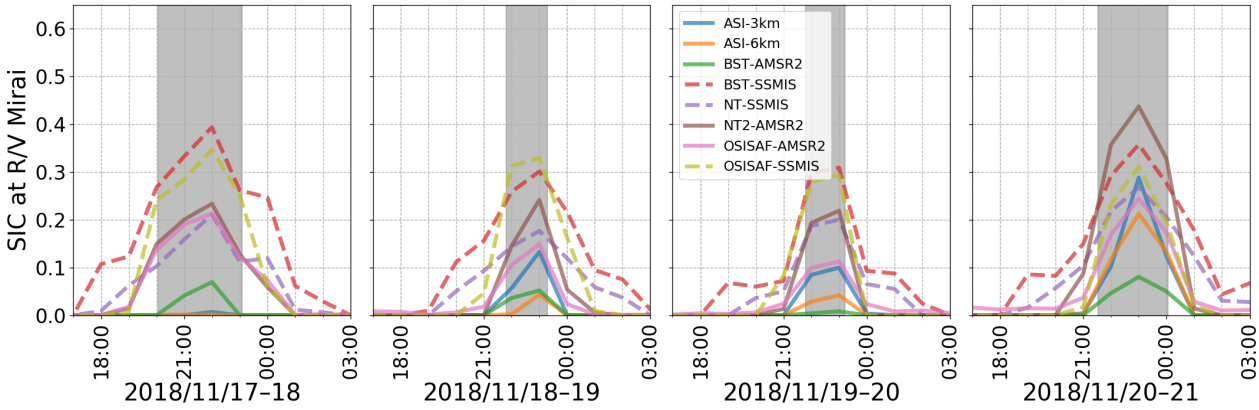

Figure A6. Satellite retrieved SIC for all products along the R/V Mirai track during Phases 3 and 4. between 17–20 November 2018. The figure schematics follow Figure A4.

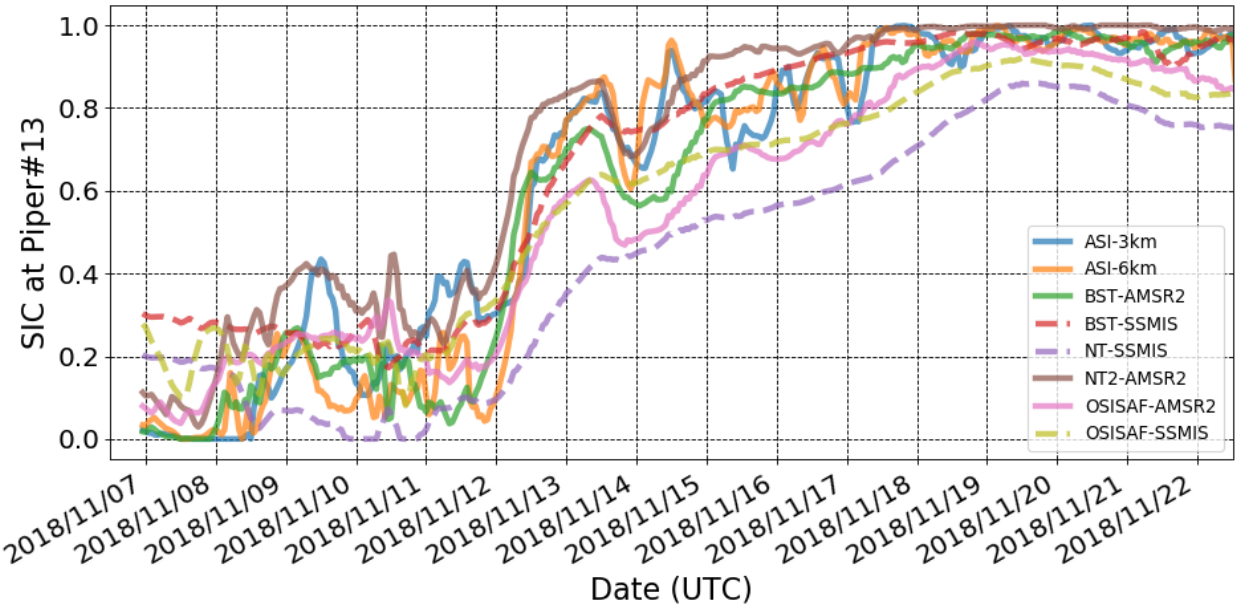

Figure A7. Satellite retrieved SIC for all products along the Piper#13 track between 7–25 November 2018. The figure schematics of SIC estimates follow Figure A4.

Table 1. Details of satellite retrieved SIC products used in this study.

Product name	Instrument	Abbreviation	Data reference (specified grid resolution)
NASA-Team (NT)	SSMIS	NT-SSMIS	Cavalieri et al. (1996) (25 km)
NASA-Team 2 (NT2)	AMSR2	NT2-AMSR2	Meier et al. (2018) (12.5 km)
Comiso-Bootstrap (BST)	SSMIS	BST-SSMIS	Comiso (2017) (25 km)
	AMSR2	BST-AMSR2	Hori et al. (2012) (10 km)
OSISAF	SSMIS	OSISAF-SSMIS	OSI-401-b: SIC product of the EUMETSAT Ocean and Sea Ice Satellite Application Facility (10 km)
	AMSR2	OSISAF-AMSR2	OSI-408: AMSR-2 SIC product of the EUMETSAT Ocean and Sea Ice Satellite Application Facility (10 km)
ARTIST-Sea-Ice (ASI)	AMSR2	ASI-6km	Spreen et al. (2008) (6.25 km Arctic grid)
	AMSR2	ASI-3km	Spreen et al. (2008) (3.125 km Chukchi-Beaufort grid)

Table 2. A list of SIC data products used for various wave-ice interaction modelling studies.

Reference	Model (wave-ice interaction parameterisation)	SIC data product
Rogers et al. (2016)	WW3 (IC3)	NASA-Team2 applied to SSMIS data and Bootstrap applied to AMSR2 data (assimilated in the sea ice model)
Cheng et al. (2017)	WW3 (IC3)	NASA-Team2 applied to AMSR2 data
Ardhuin et al. (2018)	WW3 (IC2 including IS2 scattering)	ARTIST-Sea-Ice applied AMSR2 data
Copernicus (2019)	ERA5 ECWAM (ice mask)	OSISAF applied to SSMIS data (indirectly from OSTIA (Donlon et al., 2012))
ARCMFC (2019)	ARCMFC wave model (Sutherland et al., 2019) (implemented from December 2018)	OSISAF applied to SSMIS data (assimilated in the sea ice model)